KLINIK FÜR ORTHOPÄDIE UND SPORTORTHOPÄDIE DER

TECHNISCHEN UNIVERSITÄT MÜNCHEN

KLINIKUM RECHTS DER ISAR

(DIREKTOR: PROF. DR. RÜDIGER VON EISENHART-ROTHE)

Influence of Anticoagulant Medication on Fracture-Healing using a Rat closed Fracture Model: A Morphological and Biomechanical Evaluation

Peter Michael Prodinger

TECHNISCHE UNIVERSITÄT MÜNCHEN

Klinik und Poliklinik für Orthopädie und Sportorthopädie

Klinikum rechts der Isar

Influence of Anticoagulant Medication on Fracture-Healing using a Rat closed Fracture Model: A Morphological and Biomechanical Evaluation

Peter Michael Prodinger

Vollständiger Abdruck der von der Fakultät für Medizin der Technischen Universität München zur Erlangung des akademischen Grades eines

Doktors der Medizin

genehmigten Dissertation.

Vorsitzender: Univ.-Prof. Dr. E. J. Rummeny

Prüfer der Dissertation:

1. Priv.-Doz. Dr. R. H. H. Burgkart
2. Univ.-Prof. Dr. R. von Eisenhart-Rothe

Die Dissertation wurde am 28.02.2013 bei der Technischen Universität München eingereicht und durch die Fakultät für Medizin am 17.07.2013 angenommen.

TABLE OF CONTENT

I. Abbreviations

BMC	Bone mineral content
BMP-2	Bone morphogenetic protein 2
BS	Bone surface
BV	Bone volume
DA	Degree of anisotropy
Da	Dalton
DNA	Deoxyribonucleic acid
FELASA	Federation of European Laboratory Animal Science Associations
HEPA	High efficiency particulate airfilter
IPL	Image processing language
KN	Kilo Newton
LMWH(s)	Low-molecular weight heparin(s)
mRNA	Messenger ribonucleic acid
MSC(s)	Mesenchymal stem cell(s)
NSAID(s)	Non steroidal anti inflammatory drug(s)
OTC	Over the counter
PA	Picture amplifier
Pa	Pascal
PGE-2	Prostaglandin E-2
PGF-2a	Prostaglandin F-2a
ROI	Region of interest
Runx2	Runt-related transcription factor 2
SaOS2	Sarcoma osteogenic
SMI	Structure model index
Tb. Th.	Trabecular thickness
TMD	Tissue mineral density
UK	United Kingdom

VOI	Volume of interest
V-max	Failure load
3-D	Three-dimensional
µ-CT	Micro computer tomography

II. Figures

III. Tables

IV. Introduction

Bone Healing

The process of bone healing resembles one of the most complex cascades of physiological events finally resulting in the restoration of fractured bone. It is characterized by the absence of scar formation with the final outcome ideally resembling the previous state before the fracture. This capacity is unique concerning mammalian tissues and depicts the large regenerative potential of bone up to senescence.

Bone healing demands the coordination of different cell types guided by local changes of the biochemical environment caused by the fracture and the activation of specific signal pathways. Biological changes start with the disruption of supplying vessels, the consecutive formation of the fracture-hematoma, local hypoxemia and inflammation [19]. First local growth factor release, cytokines and pro-inflammatory stimuli result in high production of prostaglandins [80]. Mesenchymal stem cells (MSCs) are stimulated to migrate, accumulate and proliferate by environmental changes, finally reaching adequate numbers to support differentiation [22, 79]. Further growth factor and prostaglandin production induces neovasculogenesis and promotes the differentiation of MSCs towards chondrogenic and osteogenic lineages, initially forming woven bone and in continuity with the hard callus [28]. The process is completed by the last and protracted period of remodeling, when resorption and new bone formation finally result in the restoration of the mechanical strength and stability of bone [14].

The outcome of this process is influenced by a diversity of local and systemic factors with varying degrees of involvement. Local inhibitory factors include the presence of a large fracture gap, disturbances of blood flow, concomitant infection, especially in case of open fractures, and extensive soft tissue damage [3]. The surgical technique, the type of stabilization and the success of the fixation are also factors which affect the fracture healing response. Insufficient mechanical stability has a negative effect on healing, resulting either in excessive or diminutive callus formation and leading to hypertrophic or hypotrophic non-unions [3, 12, 100]. Additionally, the age, gender, smoking habits and accompanying pathologies of the patient as well as the nutritional and metabolic state contribute to the delay or diminution of healing [16, 73]. Ultimately and in the centre of interest, the administration of different pharmacological agents is known to have effects on the fracture healing process [78].

Bone Healing and Medication

Several chemotherapeutic agents have been proven to draw negative impact on bone-healing in animal studies and clinical trials [8, 26, 39, 78, 90]. Their cytotoxic and anti-proliferative properties influence neovasculogenesis [38] and proper callus formation resulting in higher non-union rates [50].

Corticosteroides induce osteoporosis and are by far the most common agent causing secondary osteoporosis. Whilst the effect on bone metabolism is well explored, studies on the inhibitory effect in fracture healing have shown inconsistent results [2, 59, 78]. The reason for the differing results is still unknown and might be caused by a dose dependant effect of cortisone on bone [45]. Additionally, endochondral ossification seems clearly retarded in rats treated with cortisone whereas membranous ossification seems not affected, which complicates comparability between different animal-models and implication of experimental results towards the human situation [1].

In the clinical setting of a patient suffering a fractured bone, neither cytotoxic agents nor corticosteroids would be applied broadly and are of minor importance. What might be part of the therapeutic regiment are NSAIDs and antibiotics, both potentially affecting the process of fracture healing.

Prostaglandin E-2 (PGE-2) and Prostaglandin F-2a (PGF-2a) are known to stimulate bone formation and increase bone mass[60]. A fracture leads to high local prostaglandin production and release [18] and experimental models showed that local administration of exogenous prostaglandins can stimulate bone formation [49]. NSAIDs frequently used for pain relief and anti-inflammatory effects interfere with the local prostaglandin production and were therefore suspected to impair fracture healing. In preclinical research numerous publications using different, merely rodent animal models suggested that administration of NSAIDs correlated with various degrees of bone healing impairment [53, 57]. As other authors on the other hand demonstrated that NSAIDS have little or no effect, the situation remains unclear [77]. In humans, the potential relationship between bone healing and NSAIDs is not well explored. To summarize, the short time administration appears not to show any deleterious effects on bone but some authors stated an increased risk of developing non-union in high doses or long-term postoperative use of NSAIDs [17, 32, 82].

Several studies support the adverse effects of antibiotics on bone healing. Especially Quinolones are thought to cause chondrocyte death and therefore provide negative effects on bone healing via impairment of enchondral ossification [74, 95]. Furthermore Gentamycine and Tetracycline showed decreased bone formation in a rat animal model [51].

Bone Healing and Anticoagulation

The immobilized patient after orthopedic surgery or trauma is obligatory subject of anticoagulant therapy to prevent thrombosis or pulmonary embolism. In the absence of thromboprophylaxis, the rate of deep vein thrombosis following major lower extremity orthopedic surgery would be between 40-60%, while the risk of developing fatal pulmonary embolism reaches 1-2% [13, 97]. Established treatment includes heparin and low-molecular weight heparins (LMWHs), whilst Vitamin K antagonists (4-hydroxycoumarin-derivatives) are routinely used as anticoagulants to prevent thrombosis and embolism in cardiac arrhythmia or as long term secondary prophylaxis after thromboembolic events. Recently, Rivaroxaban was approved for the prevention of venous thromboembolism in adult patients undergoing elective hip and knee replacement surgery [24].

The potential effect of anticoagulants on fracture healing was first studied in 1955 by Stinchfield et al., prompted by the observation of high pseudoarthrosis-rates in patients receiving postoperative anticoagulant therapy for thrombophlebitis [92]. In the study, Stinchfield was able to reproduce delayed unions in animals receiving heparin. Thereafter several preclinical animal studies stated heparin and LMWH to cause decreased trabecular volume through increased resorption, a decreased rate of bone formation and lower calcification of the callus as well as delayed remodeling, presumably caused by direct osteoclast stimulation [11, 61, 64-65, 85, 94]. Street et al. showed that the administration of the newer generation anticoagulants (LMWH) resulted in the development of less mature bone with reduced torsional strength in rats, but this effect was milder compared to that of unfractioned heparin [65, 94]. Recent animal studies were not able to reproduce the postulated effect of LMWHs on fracture healing [35, 52].

Long term administration of LMWH was accused to negatively affect bone and some have associated their use with a higher risk of developing osteoporosis [81]. Although heparin-induced osteoporosis represents a rare adverse effect of LMWH treatment, the incidence should be around 2-5% [98]. Prolonged, unfractionated heparin treatment is associated with bone loss and an increased risk of fracture [15, 91]. As present in fracture-healing, there is some evidence to suggest that LMWHs may have a reduced incidence of osteopenia and osteoporosis compared with unfractionated heparin [81].

Concerning the administration of Vitamin K antagonists, Dodds et al. showed a decrease in periosteal activities of glucose 6-phosphate dehydrogenase and of alkaline phosphatase around fractures in rats, indicating that also Vitamin K-antagonists influence the bone metabolism in fresh callus tissue [20].

Bone Healing and direct Factor Xa-Inhibition by Rivaroxaban

Systematic examinations on the possible effects of the direct factor Xa-inhibitor Rivaroxaban on bone healing are sparse. Solayer et al. treated primary human osteoblast cultures *in vitro* with varying concentrations of Rivaroxaban and Enoxaparin and found a significant, dose independent reduction in osteoblast function measured by alkaline phosphatase activity. This reduction was associated with reduced mRNA expression of the bone marker osteocalcin, the transcription factor Runx2, and the osteogenic factor BMP-2. Though both agents did not adversely affect osteoblast viability, the authors concluded that rivaroxaban treatment may negatively affect bone through a reduction in osteoblast function [89]. Similarly Gigi et al. observed a dose-dependent inhibition of the DNA-synthesis and Creatine kinase-specific activity of SaOS2 cells via Rivaroxaban. Alkaline phosphatase-specific activity was less- and cell mineralization unaffected. The in vitro model demonstrated a significant Rivaroxaban-induced reduction in osteoblastic cell growth and energy metabolism and these findings might indicate that Rivaroxaban inhibits the first stage of bone formation [31].

Objectives

As new bone formation or bone healing resembles a complex cascade of various sequences, demanding the coordination of different cell types and the activation of specific signal pathways, a single cell culture might not be sufficient to comprehend the whole process finally resulting in the restoration of bone. In light of the fact that heparin and LMWHs have been associated with adverse effects on bone and the risk of developing osteoporosis on the one hand and the possible inhibitory effects of Rivaroxaban, deduced by the results of the above mentioned *in vitro* studies on the other, we attempted to investigate those *in vivo* via a standardized, rodent fracture model. The effect of each agent (Rivaroxaban and Enoxaparin) was evaluated in terms of biomechanical properties and morphological alterations of the formed callus.

Derived questions were as follows:

1) Does anticoagulant medication (Rivaroxaban or Enoxaparin) alter the biomechanical properties of new-formed callus *in vivo*?
2) Are there any morphological changes of the callus under the influence of anticoagulant medication *in vivo*?
3) If yes, do these changes correspond to biomechanical incompetence?

V. Material and Methods

The study was performed in the animal facility of the Klinikum rechts der Isar, Technische Universität München and was evaluated and approved by the local authority (Regierung von Oberbayern, approval no. 55.2-1-54-2531-17-10) as required by German law. The facility is registered as a breeding and experimental facility according to §11 Tierschutzgesetz, which harmonizes national legislation with the European Community Directive 86/609/EEC on the protection of animals used for experimental and other scientific purposes. Rats were maintained according to the relevant recommendations of the Appendix A of the European Convention (ETS No. 123).

Animals and Housing

For the study (main experiment and two pilot studies) male Wistar rats, 15 weeks of age (Charles River Laboratories, Sulzfeld, Deutschland, CRL:WI) were used. After arrival, all rats were granted a 14 day acclimatization period before entering the experiment. Rats were housed in open cages, polysulfone type III OTC, with a base area of 825 cm^2 (Ehret, Emmendingen, Germany). Although rats are social animals, differences in rank might influence the amount, frequency and point in time of food uptake. With feed being the route of administration for Rivaroxaban, all rats were single housed in order to exclude possible effects of such kind on the data.

Environment

All cages were kept at a room temperature of 21 ± 1 °C, relative humidity of 45 - 65% and a light regime of 12:12 - hour light : dark cycle (lights on 0600 to 1800) with a dimming phase of 30 minutes. In order to maintain particulate cleanliness, room air supply was HEPA filtered and a positive air pressure of 60 Pa was kept within the room. In order to enter the animal housing area, personnel has to change from street-wear into scrubs, which is performed outside the animal area. Before entering the animal room, hands and arms are disinfected and additional protective clothing such as a disposable sterile uniform, mask, cap, gloves, and shoe covers is donned.

Food and Water

All rats had ad-libidum access to tap water in drinking bottles. Food consisted of pelleted maintenance diet for rats and mice (item no. 1320, Altromin, Lage, Germany). Rats treated with Rivaroxaban were fed with medicated feed provided by Bayer Health Care AG. Due to its floury consistency, Rivaroxaban feed was fed using a special feeder that was placed and fixated inside the cage. In order to allow acclimatization to the floury texture of feed and the feeder itself, feed containing no drug was offered using the feeder for 10 days before entering the experiment.

Bedding

The bedding in each cage consisted of softwood fibers (Lignocel 3-4, Sniff, Soest, Germany). Cages and bedding were changed once each week.

Enrichment

Rat Corner homes (Datesand, Manchester, UK) and autoclaved hay were offered as enrichment.

Health Monitoring

All rats in the facility were screened regularly by using a sentinel health monitoring program, in accordance to the Federation of European Laboratory Animal Science Associations (FELASA) recommendations, and were free from a wide range of pathogens including Kilham rat virus, rat parvovirus, Toolan H1 virus, Sendai virus, pneumonia virus of mice, reovirus, murine encephalomyelitis virus, sialodacryoadenitis virus, rat minute virus, Hantaan virus, lymphocytic choriomeningitis virus, cilia-associated respiratory bacillus, mouse adenovirus types 1 and 2, rat rotavirus, rat coronavirus, Mycoplasma pulmonis, Clostridium piliforme, Bordetella bronchiseptica, Pasteurella spp., fur mites, and pinworms.

Animal Care Procedure

All rats were granted a 14 day acclimatization period before entering the experiment or one of the pilot tests. Over the 21 day study period, rats were monitored for clinical signs of illness and signs of pain or distress. Animals were monitored twice daily for 3 days postoperatively and thereafter by once-daily visual observation and at every weighing. All monitorings, postoperative analgesic management, application of test-substances and fluorochromes were conducted by the same people (Veterinarians Martina Knödler and Gabriele Wexel) throughout the duration of the experiment to ensure consistent

environmental factors. Animal care staff was acquainted with the characteristics of the experiment and informed about possible complications and their symptoms. At least one of the veterinarians was available for animal care staff by telephone at any time during the experiment.

Pilot Study I

Objectives

The main objective of pilot study 1 was the determination of plasma levels and factor Xa-inhibition for both, Rivaroxaban and Enoxaparine to achieve comparable levels during the main experiment. A first dose-equivalent for Rivaroxaban was calculated on the basis of prior experience provided by Bayer Health Care AG, as well as on the basis of extrapolations of dosages used in humans. For Enoxaparine, a dose equivalent was calculated on the basis of data provided by relevant literature [85, 94].

The second objective of pilot study 1 was determination of possible changes in Rivaroxaban plasma levels / factor Xa-inhibition in the operative setting. Especially concerning the oral administration of Rivaroxaban, altered food-intake of the animals postoperatively would provide direct impact on the main target of the study, therefore constant homogenous and comparable distribution of the pharmaca in the experimental situation had to be ensured.

Methods

For plasma level measurements of both Rivaroxaban and Enoxaparin 10 rats were used in this pilot, whereas one rat (number 10) served as a control. In order to evaluate the effects of the surgical intervention on food uptake, rats receiving Rivaroxaban were divided into two groups. Rats 1-3 did not undergo surgery. In rats 4-6 surgery was conducted in accordance with the main study and blood samples were collected during the postoperative period. Enoxaparin was administered once daily by subcutaneous injection of 250 IU/kg. Rivaroxaban was administered by medicated feed at a dosage of 1000 ppm.

List of animals:

1	Rivaroxaban	no surgery	**4**	Rivaroxaban	after surgery
2	Rivaroxaban	no surgery	**5**	Rivaroxaban	after surgery
3	Rivaroxaban	no surgery	**6**	Rivaroxaban	after surgery
7	Enoxaparin		**10**	Control	
8	Enoxaparin				
9	Enoxaparin				

All rats received either the Rivaroxaban enriched fed or Enoxaparin at 10 am in the morning.

Rats 1-3

Rats 1, 2 and 3 were offered Rivaroxaban feed at a dosage of 1000 ppm starting at 10 am on Tuesday 25th of January 2011. Three blood samples were taken at an interval of 8 hours.

Rivaroxaban feed	10 am	(Tuesday, January 25th 2011)
1. Blood sample	6 pm	(Tuesday, January 25th 2011)
2. Blood sample	2 am	(Wednesday, January 26th 2011)
3. Blood sample	10 am	(Wednesday, January 26th 2011)

Rats 4-6

Rats 4, 5 and 6 were offered Rivaroxaban at 10 am on Tuesday, 25th of January 2011. Surgery according to the main study was performed between noon and 2 pm the same day. For reasons of standardisation, surgical intervention was performed by one person only. Therefore, rats 4, 5 and 6 underwent surgery at different times of the day. As a consequence, whilst still at an interval of 8 hours, blood samples were taken at different times of the day as well.

Rats 7-9

Rats 7, 8 and 9 were administered Enoxaparin subcutaneously at a dosage of 250 IU/kg at 4 pm on Tuesday, 25th of January. The first blood sample was taken 2 hours after injection of Enoxaparin, all following blood samples were taken at an interval of 8 hours.

Enoxaparin injection	4 pm	(Tuesday, January 25th 2011)
1. Blood sample	6 pm	(Tuesday, January 25th 2011)
2. Blood sample	2 am	(Wednesday, January 26th 2011)
3. Blood sample	10 am	(Wednesday, January 26th 2011)

Rat 10

Rat 10 received 1 ml of sterile NaCl at 10 am. Blood samples were taken at an interval of 8 hours.

1. Blood sample 6 pm (Tuesday, January 25th 2011)

2. Blood sample 2 am (Wednesday, January 26th 2011)

3. Blood sample 10 am Wednesday, January 26th 2011)

Plasma levels of Rivaroxaban and Enoxaparin were evaluated by the Bayer Health Care AG. Furthermore, activity of endogenous factor Xa was determined and a calibration curve was established using a Hyphen Assay, which was modified by Bayer Health Care AG. Plasma levels were then converted into percentage of factor Xa-inhibition using a calibration curve. The percentage of Factor Xa-inhibition in the test samples was then evaluated using the calibration curve.

Results

The results of every animal at each depicted time-point are summarized in **Tables 1 to 3** and **Figures 1 and 2**.

The analysis of the data revealed a highly different degree of factor Xa-inhibition between enoxaprine and rivaroxaban. Since factor Xa inhibition levels were extremely high, specimens had to be diluted 1:10 and the measurements were repeated with the diluted samples. 4 hours after administration, factor Xa-inhibition measured between 44 and 62 % for Rivaroxaban (diluted sample), whereas in rat number 4 levels were as low as 11 %. We link this to the fact that this particular animal showed a poor general condition postoperatively that might have been the consequence of a longer duration of the surgical intervention. In comparison, 250 IU/kg of Enoxaparin only resulted in 8-13 % of factor Xa-inhibition (diluted sample).

Table 1:

Rat Nr.	Substance	OP	Dilution of plasma	% FXa-Inhibiton
1/1	Rivaroxaban	pre	1:10	47
1/2				57
1/3				46
2/1	Rivaroxaban	pre	1:10	44
2/2				51
2/3				54
3/1	Rivaroxaban	pre	1:10	45
3/2				48
3/3				41
4/1	Rivaroxaban	post	1:10	11
4/2				6
4/3				1
5/1	Rivaroxaban	post	1:10	62
5/2				49
5/3				43
6/1	Rivaroxaban	post	1:10	62
6/2				27
6/3				35

Table 1: Results of factor Xa-Inhibition of animals 1 to 6 (Rivaroxaban) at different time points in the pre- and postoperative phase (%FXa-Inhibition: Percentage of Factor Xa inhibition).

Table 2:

Rat Nr.	Substance	OP	Dilution of plasma	% FXa-Inhibiton
7/1	Enoxaparin	none	1:10	8
7/2				-1
7/3				2
8/1	Enoxaparin	none	1:10	13
8/2				2
8/3				1
9/1	Enoxaparin	none	1:10	9
9/2				-3
9/3				-2

Table 2: Results of factor Xa-Inhibition of animals 7 to 9 (Enoxaparin) at different time points (no surgical intervention, dilution of plasma, %FXa-Inhibition: Percentage of Factor Xa inhibition).

Table 3:

Ratte Nr.	Substance	OP	Dilution of plasma	% FXa Inhibiton
7/1	Enoxaparin	none	none	66
7/2			none	16
7/3			none	11
8/1	Enoxaparin	none	none	68
8/2			none	11
8/3			none	-6
9/1	Enoxaparin	none	none	72
9/2			none	13
9/3			none	13

Table 3: Results of factor Xa-Inhibition of animals 7 to 9 (Enoxaparin) at different time points (no surgical intervention, no dilution of plasma, %FXa-Inhibition: Percentage of Factor Xa inhibition).

Conclusion:

Interpretation of data lead to following conclusions:

First the food uptake postoperatively under normal, postoperative circumstances with the animal in good shape and condition was predictable and therefore sufficient factor Xa-inhibition could be guaranteed for the main experiment.

Second, estimated doses for adjusting factor Xa-inhibition in both groups revealed different values, being way too high in the Rivaroxaban- and declining to fast in the Enoxaparin group. Since the originally estimated dosages showed to be insufficient, a second pilot study was planned to adjust dosages for Enoxaparin and Rivaroxaban.

Figure 1:

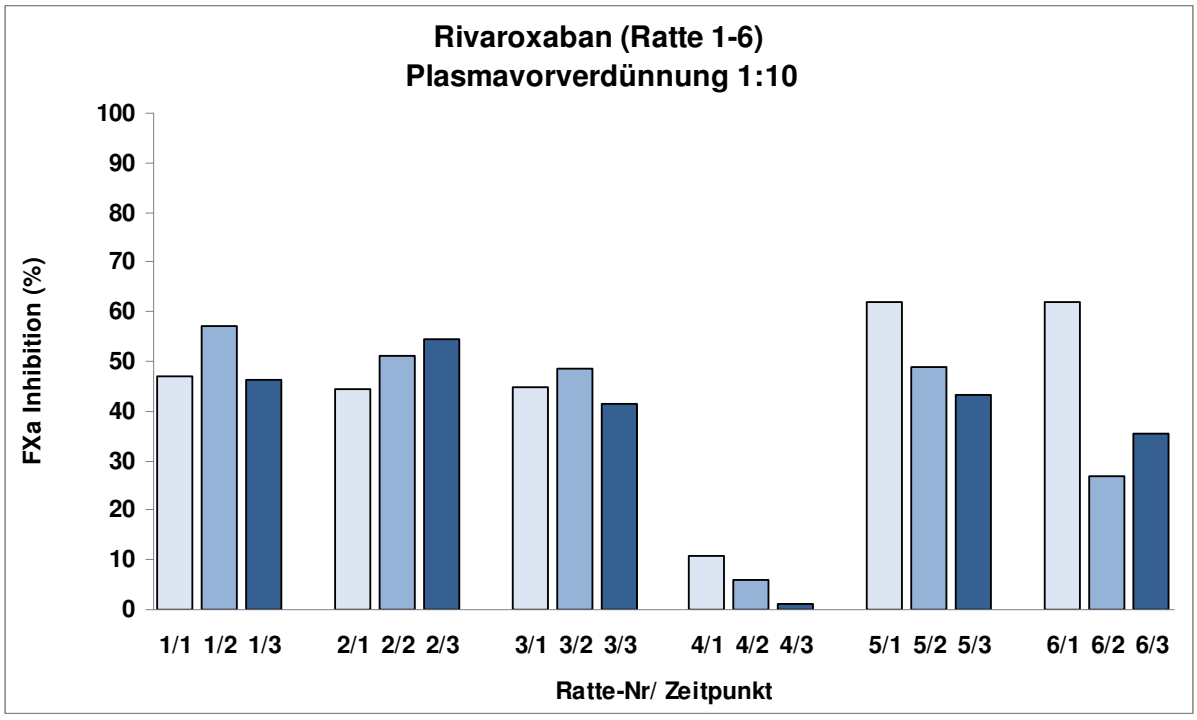

Figure 1: Results of factor Xa-Inhibition of animals 1 to 6 (Rivaroxaban) at different time points in the pre- and postoperative phase (FXa Inhibition (%): Percentage of Factor Xa Inhibition, Timepoints: -/1 = 8 hours after application, -/2 = 16 hours after application, -/3 = 24 hours after application).

Figure 2:

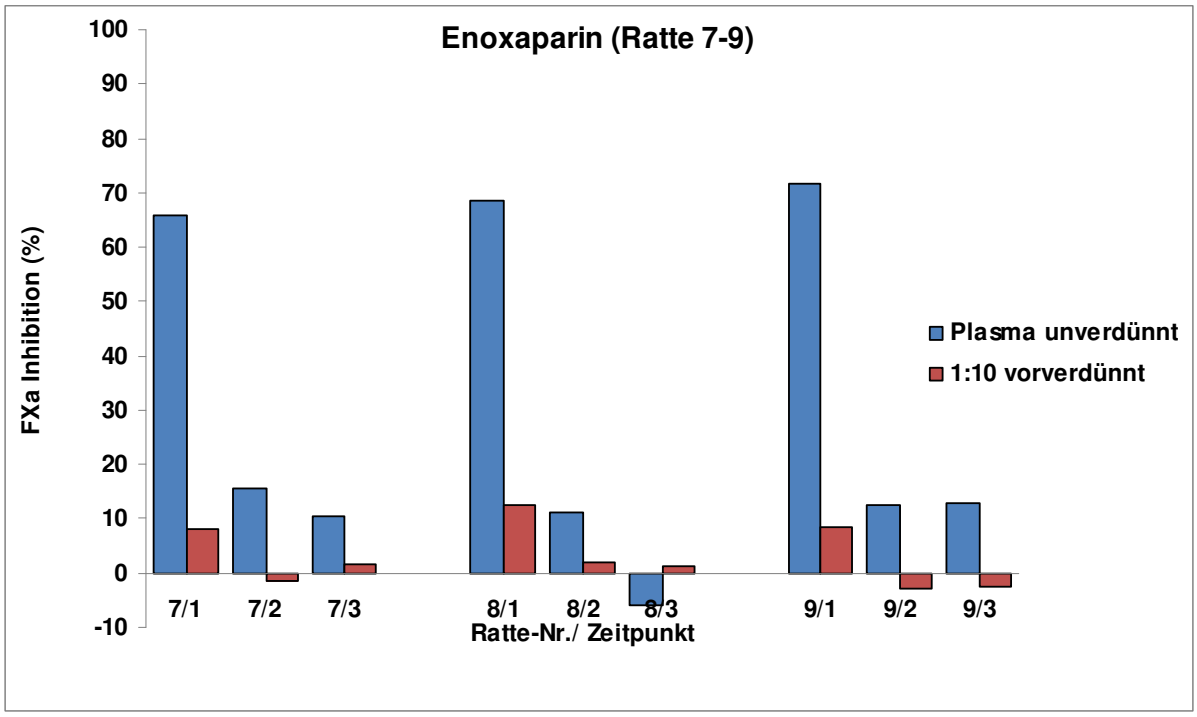

Figure 2: Results of factor Xa-Inhibition of animals 7 to 9 (Enoxaparin) at different time points (no surgical intervention, FXa Inhibition (%): Percentage of Factor Xa Inhibition, Timepoints: -/1 = 8 hours after application, -/2 = 16 hours after application, -/3 = 24 hours after application).

Pilot Study II

Objectives

As the originally estimated dosages used in Pilot Study I showed to be not suitable, dosages for both substances needed to be readjusted in order to achieve a comparable level of factor Xa-inhibition. Therefore we planned to assess factor Xa-inhibition using different amounts of Enoxaparin measured at different time-points in comparison to rats receiving Rivaroxaban feed containing 600 ppm of the substance.

Methods

In this Pilot, a total number of 11 rats were used, whereas 6 rats (rats 1-6) were administered Enoxaparine and 5 rats (rats 7-11) were fed Rivaroxaban at the dosages shown below.

List of animals:

1	350 IU/kg subcutaneously	**7**	600 ppm Rivaroxaban
2	350 IU/kg subcutaneously	**8**	600 ppm Rivaroxaban
3	500 IU/kg subcutaneously	**9**	600 ppm Rivaorxaban
4	500 IU/kg subcutaneously	**10**	600 ppm Rivaroxaban
5	1000 IU/kg subcutaneously	**11**	600 ppm Rivaroxaban
6	1000 IU/kg subcutaneously		

With Enoxaparin being administered subcutaneously, it was necessary to monitor pharmacokinetic properties closely to adjust dosage and frequency of applications. This was achieved by frequent measurements over time as shown below (**Figures 3 and 4**):

Figure 3:

Illustration of blood sampling over time for Rivaroxaban

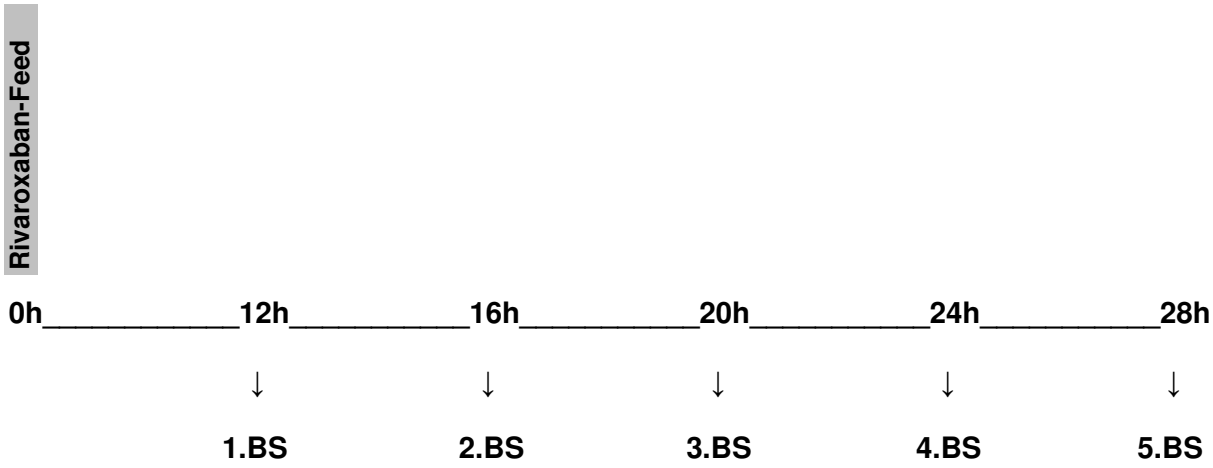

BS = blood sample

1. BS 2 pm local time
2. BS 6 pm local time
3. BS 10 pm local time
4. BS 2 am local time
5. BS 6 am local time

Figure 3: Blood samples were collected from rats 7 – 11 as outlined above. The first blood sample was collected 12 h after administration of Rivaroxaban-feed. All subsequent blood samples were taken at intervals of 4 h.

Figure 4:

Illustration of blood sampling over time for enoxaparin

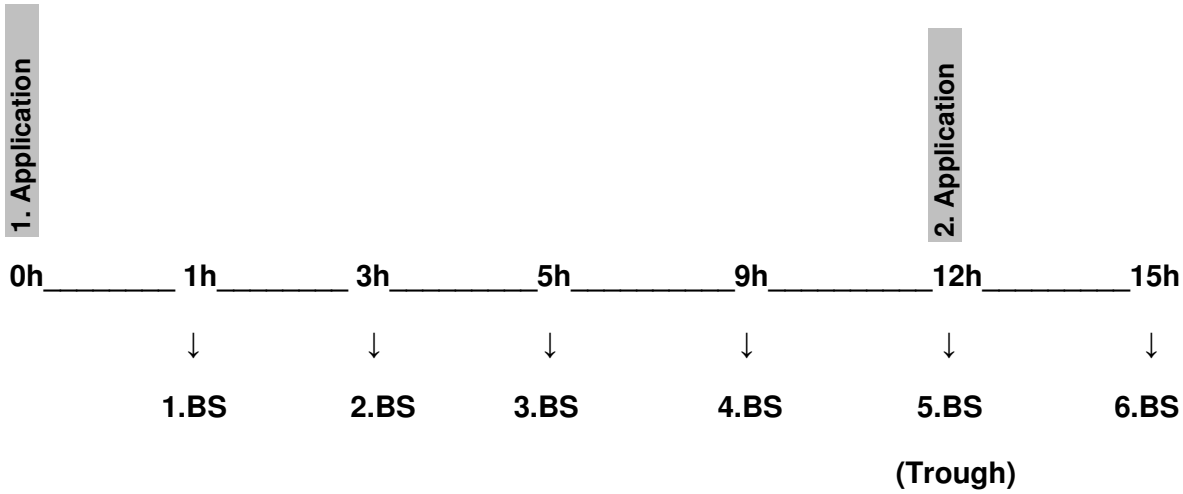

BS = blood sample

2 Rats 350 IU/kg subcutaneously (Rat 1 and 2)
2 Rats 500 IU/kg subcutaneously (Rat 3 and 4)
2 Rats 1000 IU/kg subcutaneously (Rat 5 and 6)

Figure 4: Blood was drawn from rats 1-6 as outlined above. The first administration of Enoxaparin was performed at 0h. The first blood sample (BD) was collected 1h after initial administration of Enoxaparin, with following blood samples at time points 3h, 5h and 9h. The 5th blood sample was collected immediately prior to the second application of Enoxaparin at 12h for determination of through levels.

Results

Levels of factor Xa-inhibition were evaluated by the Bayer Health Care AG using the calibration curve that was established during Pilot Study I and are displayed in **Tables 4 to 6** and **Figures 5 and 6**.

Table 4:

	Time after injection (h) / FXa-Inhibition (%) mean					
Enoxaparin (no dilution of plasma)	1 h	3 h	5 h	9 h	12 h	15 h
350 IU/kg	53	55	39	17	-1	53
500 IU/kg	60	68	58	24	8	59
1000 IU/kg	76	80	74	35	5	76

Table 4: Inhibition of factor Xa with different amounts of Enoxaparin measured at different time-points.

Table 5:

	Time (h) / FXa Inhibition (%) mean				
Rivaroxaban (600 ppm)	12 h	16 h	20 h	24 h	28 h
No dilution of plasma	84	86	89	90	85
SD (1:10)	7	5	3	1	3

Table 5: Inhibition of factor Xa with 600 ppm Rivaroxaban measured at different time-points.

Table 6:

	Time (h) / FXa Inhibition (%) mean				
Rivaroxaban (600 ppm)	12 h	16 h	20 h	24 h	28 h
1:5 dilution	26	31	38	39	29
SD (1:10)	9	8	5	5	8

Table 6: Inhibition of factor Xa with 600 ppm Rivaroxaban measured at different time-points.

Figure 5:

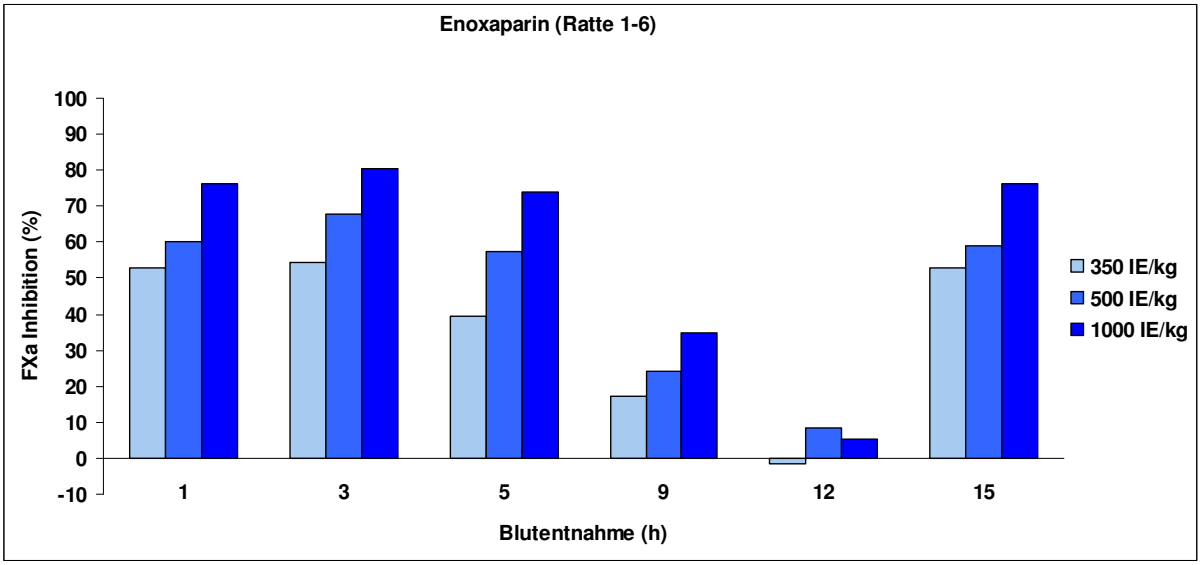

Figure 5: Inhibition of factor Xa with different amounts of Enoxaparin measured at different time-points (1, 3, 5… hours after application).

Figure 6:

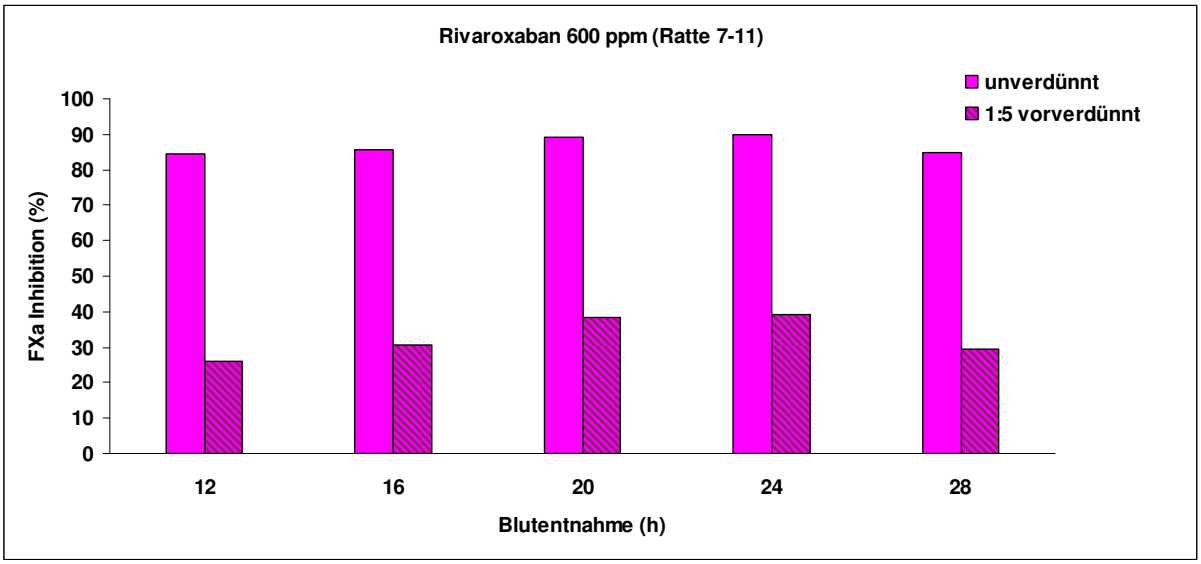

Figure 6: Inhibition of factor Xa with 600 ppm Rivaroxaban measured at different time-points (12, 16, 20… hours after application of enriched fed).

Conclusion

The analysis of the data revealed that 600 ppm of Rivaroxaban lead to a constant level of factor Xa-inhibition that was comparable to the level produced by 1000 IU/kg Enoxaparin. Inhibition levels were between 84% and 90 % for Rivaroxaban measured over a period of 16 hours. Although Enoxaparin produced comparable levels of factor Xa-inhibition ranging from 74% to 80 % in the first 4-5 hours after injection, efficiency was decreasing between 5 and 9 hours after injection.

12 hours after injection of Enoxaparin, inhibition of Factor Xa was not measurable. Therefore, it was agreed upon, to administer Enoxaparin twice daily every 12 h in the main study.

Main Experiment

70 male Wistar rats (CRL:WI), obtained from Charles River Laboratories (Sulzfeld, Germany), 15 weeks of age and weighing between 380 and 480g were used in the main experiment. After acclimatisation they were randomized and allocated to the different arms (Enoxaparin, Rivaroxaban and Control) and groups (Group A: Morphometry, 7 animals per substance; Group B: Biomechanical Testing, 15 animals per substance; 4 reserve) of the study. They were operated in sense of antegrade pinning of the right femur and a standardized fracture was done subsequently. After 21 days the animals were euthanized and both femora harvested. According to group-allocation the bones were fixed in 100% Methanol (Group A) and stored at 4°C or fresh frozen and stored at -20°C. Analyses were done via biomechanical testing until failure or Micro CT scan.

Randomization and Blinding

Animals were divided into 6 groups:

	Rivaroxaban	Enoxaparin	Control
(Group A) Morphometry	7 rats	7 rats	7 rats
(Group B) Biomechanical testing	15 rats	15 rats	15 rats

The animals were randomized and allocated either to Rivaroxaban, Enoxaparin or controls. A second randomisation was done to determine animals for biomechanical testing or morphological analysis.

Randomization was performed by veterinarian Martina Knödler, instead of having been computer-generated. This type of randomization was chosen to avoid unintentional bias. As the surgery was conducted on 10 different dates, we chose to equally include animals of every substance on each of the surgery dates. Therefore, any day-dependant influences would not create an unintentional bias.

All researchers conducting surgery, performing x-rays, collecting samples or analyzing data were blinded throughout the duration of the entire experiment.

Application of Medication

Enoxaparin was administered twice daily (every 12 hours) with 1000IU/kg body weight starting with the first injection 12 hours before the operation.

Rivaroxaban was fed with medicated feed provided by Bayer Health Care AG, containing 600 ppm/g. The medicated fed was applied 24 hours before the operation.

The chosen amount of medication and application has proven to produce comparable levels of factor Xa inhibition.

Anesthesia and Preoperative Preparations

Anesthesia was induced intramuscularly using a combination of midazolam (DORMICUM® 2mg/kg), medetomidine (DOMITOR® 0,15mg/kg) and fentanyl (FENTANYL® 0,005mg/kg). The degree of analgesia produced by medetomidine in combination with the potent opioid fentanyl is sufficient for this procedure. A third analgesic component, metamizol, was administered orally before induction of anesthesia (see postoperative analgesia). As this particular anesthesia is completely reversible, long recovery periods are avoided, which minimizes complications such as hypoglycemia. Animals breathed spontaneously during anesthesia. The inspired room air was supplemented by flow of oxygen provided by a mask positioned in front of nose and mouth. Monitoring of pulse rate and peripheral arterial oxygen saturation was conducted using pulse oxymetry. After induction of anesthesia, all rats received a subcutaneous injection of NaCl (5 ml) which, being slowly absorbed, has the effect of a slow intravenous infusion. The complete right hind limb and the lower part of the body were shaved. Bepanthen® Augen- und Nasensalbe was used to protect the cornea from drying out during anesthesia. In order to prevent hypothermia, a heating mat was placed on the surgery table, which was then covered with a sterile drape. After positioning the rat on the surgical table, the previously shaved area including the complete hind limb was desinfected using Cutasept® F (Bode Chemie GmbH, Hamburg) and a sterile fenestrated sheet was positioned.

At the end of the procedure, anesthesia was reversed by a subcutaneous injection of atipamezole (ANTISEDAN, 0,75mg/kg) and flumazenil (ANEXATE 0,2mg/kg). Since buprenorphine was used for postoperative analgesia, we decided not to reverse fentanyl. Buprenorphine itself, possessing a higher receptor affinity than fentanyl, will lead to displacement of fentanyl from the opioid receptor.

Intramedullary Pinning

The operative procedure was performed as modification of the method first described by Bonnarens and Einhorn in 1984 [6]. Instead of opening the knee joint for retrograde pinning, the K-wire was inserted anterograde via the intertrochanteric fossa.

All animals were prepared for surgery by shaving and cleansing of the left leg. After preoperative skin-desinfection, sterile coverage of the op-site was provided. The skin incision was done over the greater trochanter. After cutting the fascia, the gluteal muscles were separated respecting the direction of fibers. The intertrochanteric fossa was palpated and the femoral neck was grasped with a curved forceps. Subsequently a 0.6mm K-wire was drilled into the intramedullary cavity by the use of a PA. Distally, the pin reached the supracondylar region without exceeding the bone, so as not to interfere with knee motion. After a terminatory radiographic control in 2 planes, the pin was cut flush with the cortex and the wound closed in layers (**Figure 7**).

Figure 7:

Figure 7: Intraoperative radiograph: Insertion of K-wire via the intertrochanteric fossa. Femoral neck grasped with a forceps.

Standardized Fracture and Device

During the same anesthesia a standardized fracture was done according to the method described by Bonnarens et al. [6]. It was accomplished by the use of a blunt guillotine 3-point bending device. This consisted of a 500 g weight driving a blunt guillotine down onto an outstretched rat leg placed across an open platform, creating a 3-point bending mechanism (**Figure 8**).

Figure 8:

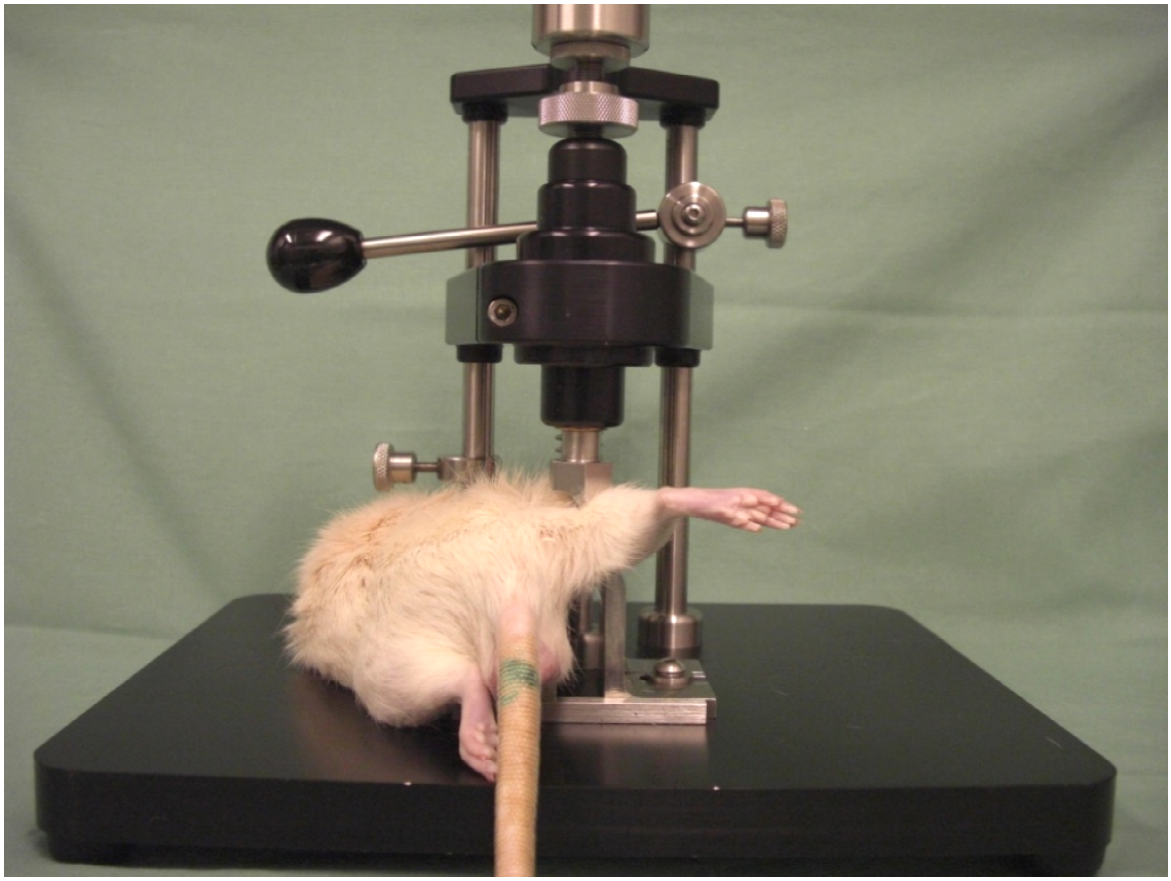

Figure 8: Anesthetized animal placed on the fracture device. Leg placed across an open platform.

The fracture system consists of four components: a frame; an animal support system; a guillotine ramming system; and a 500 g steel weight. The frame consists of a base and two platforms mounted on vertical posts. A rod is secured to the upper platform and serves as a guide for the dropped weight. The guillotine ramming system consists of an impact-disc located above the upper platform. It can be driven downward by the dropped weight. The

downward displacement of the disc is limited. The system drives a blunt guillotine blade between the anvils of the animal support stage. A spring provides just enough recoil to return the guillotine to its starting position after the dropped weight is lifted (**Figure 9**).

Figure 9:

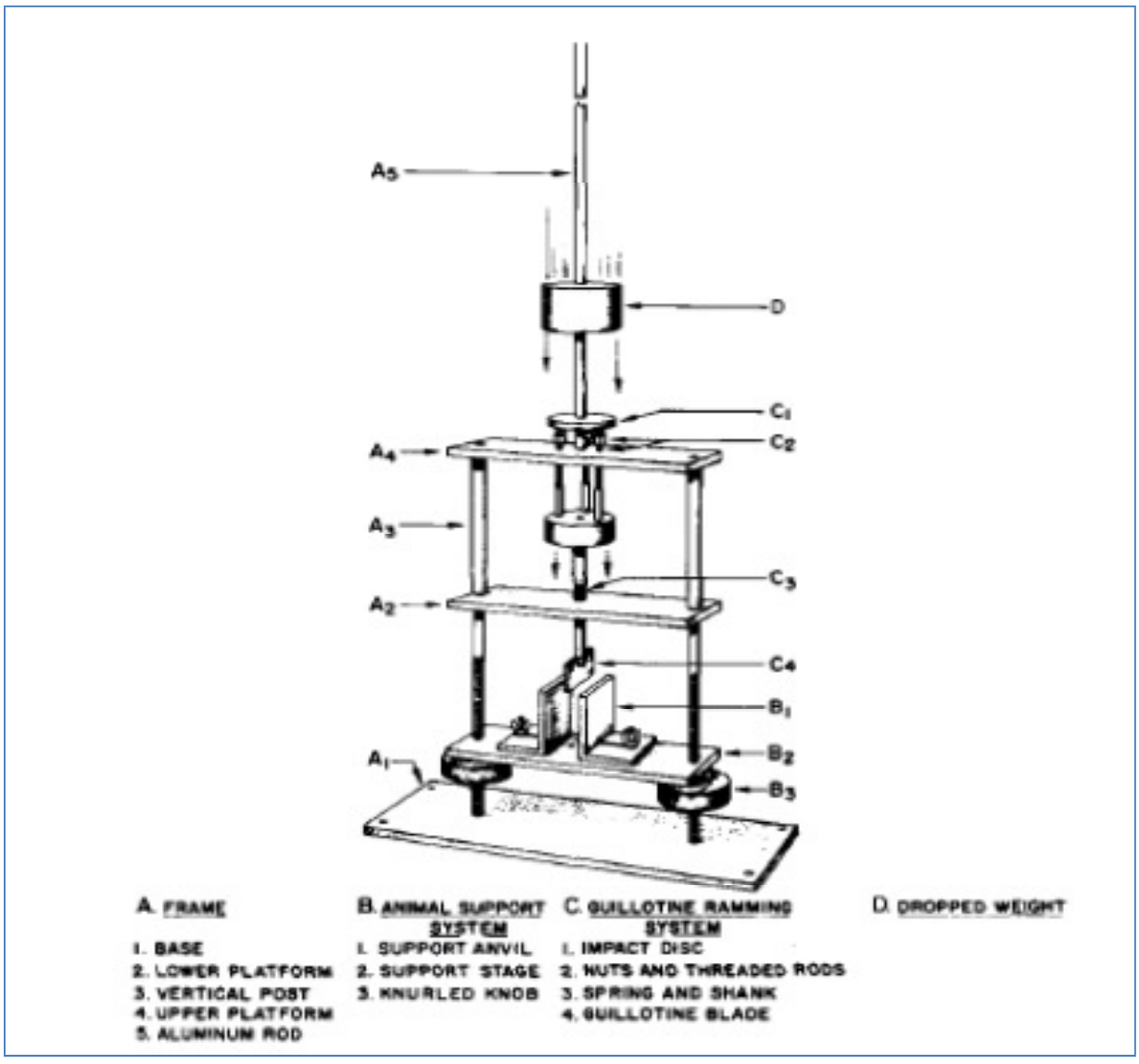

Figure 9: Systematic drawing of the fracture-apparatus [6].

With the animal supine, the prepinned femur was placed in abduction and external rotation and positioned over the center of the animal support stage. This was done so that one anvil supported the intertrochanteric region and the other the supracondylar region. The support stage was raised until the guillotine blade of the fracture device was snug with the thigh. The

travel of the ramming system was set at 1.5 mm. This distance is equivalent to one-half the diameter of the midshaft of the femur as recommended by Jackson et al. [42]. The 500 g weight was dropped from a height of 35 cm. The force of the descending weight was transmitted to the impact disc, driving the guillotine ramming system and fracturing the femoral diaphysis.

After the pinned femur was fractured, a radiograph was taken to document the fracture configuration (**Figure 10**).

Figure 10:

Figure 10: Postoperative radiographs, two planes after fracture. Same animal than in figure 7. A transverse fracture with minimal dislocation can be seen at the middle of the femoral shaft.

Postoperative Analgesia and Care

Postoperative analgesic care consisted of subcutaneous buprenorphine (TEMGESIC 0,075 mg/kg bodyweight) as well as Metamizol-Natrium (NOVAMINSULFON-RATIOPHARM TROPFEN 50 mg/kg) orally. Both substances were administered every 12 h for the first 3 days after surgery. In order to achieve continuous pain relief during surgery, recovery and postoperative period, the first dose of metamizol was administered prior to induction of anesthesia. The first dose of buprenorphine was injected during wound closure.

Consequently, a more balanced anesthetic regimen is achieved and 'analgesic gaps' between offset of anesthesia and onset of postoperative analgesics are avoided.
Woundhealing, weight-bearing of the fractured leg and bodyweight of the rats were controlled and documented throughout the whole experiment (21 days). Signs of wound-infection, extensive hematoma, protracted limping or the loss of more than 10% of the body weight would have led to termination and euthanasia of the animal.

Euthanasia

Prior to euthanasia, all rats were anesthetized using the combination of midazolam (DORMICUM® 2mg/kg), medetomidin (DOMITOR® 0,15mg/kg), fentanyl (FENTANYL® 0,005mg/kg) as described above. After achieving general anesthesia, the rats were euthanised according to the recommendation of the European Union using a threefold overdose of Phenobarbital (90mg/kg) i.v. Subsequently the lower extremities were dissected and both femura harvested. Surrounding skin, muscle, and other soft tissues were removed. Macroscopic appearance of the callus and possible malpositions of the femur were assessed and documented, a radiographic control was done in 2 planes (**Figures 11 and 12**). The bones assigned to the Micro-CT group were fixed and stored in 100% Methanol at 4°C in lightproof Falcon-tubes. Those assigned to biomechanical testing were stored at -20° C.

Figure 11:

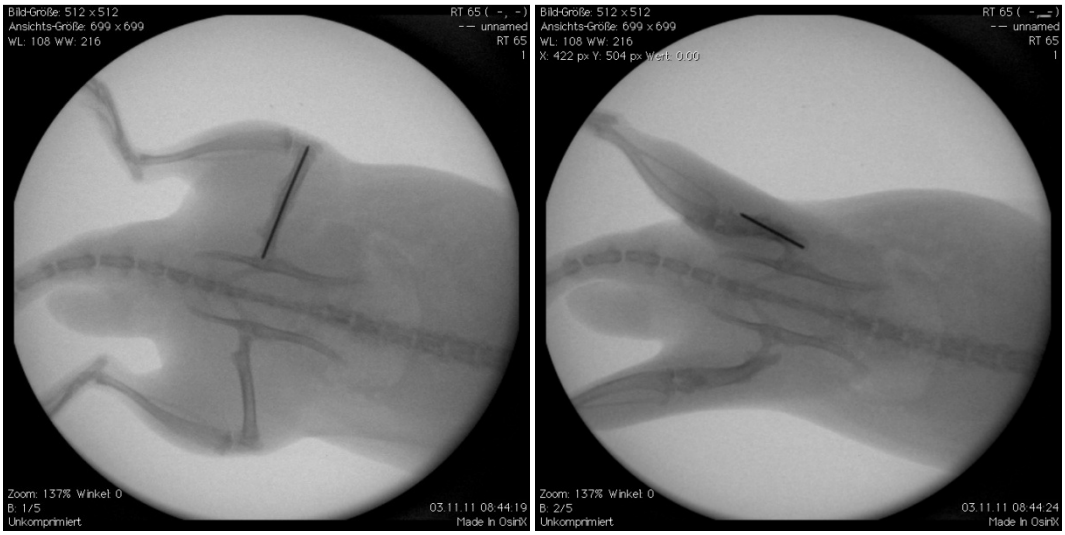

Figure 11: Radiographs, two planes at euthanasia. Same animal than in figure 7. Bridging callus.

Figure 12:

Figure 12: Macroscopic documentation of both harvested femora. Edge of the K-wire can be seen at the greater trochanter of the right femur. Bridging callus at the former fracture.

Micro CT Scan

After removal of the intramedullary pin, all femurs were imaged with a micro-CT scanner (µ-CT 40, Scanco Medical® AG, Brüttisellen, Switzerland).

Analysis via µ-CT is a non-invasive, non-destructive method which enables the examination of hard tissue up to a pixel size of 0.5 µm without the need of any specific preparation. Due to isotropic resolution, the slice thickness was consistently the same as the pixel size within one slice. By the obtained data, 3-D stereological indices were calculated which comply with standards of histomorphometric dimensions [4]. The validity and comparability of the results in comparison to other histomorphometric methods which evaluate bone architecture were confirmed in various studies [9, 67-68].

The samples were placed and aligned in parallel to a transparent cylindrical sample holder (18.5 mm diameter) and secured with a surrounding sponge [66]. For heat protection and preservation from drying the sample holder was filled with 100% methanol for the duration of the examination time of 61.9 minutes.

In preparation of each µ-CT analysis a scout view scan equivalent to an ordinary x-ray scan was used for the exact determination of the region of interest (ROI) [4]. In our study the ROI covered 6.2 mm in the z-axis, 3.1mm proximal and 3.1mm distal of the fracture gap (**Figure 13**).

Figure 13:

Figure 13: Scout view scan before µCT-measurement.

The scans with a thickness of 0.01 mm were performed with a ‚high resolution scan mode'. The integration time was set at 200ms. 1000 projections (each projection is sampled for 200 ms) with 2048 measurement points each were taken over 180°. The integration time corresponds to the exposition time of the detector of the x-ray of each projection is exposed to. We scanned 620 slices for each specimen. After the reconstruction of the data the analysis of the micro-structural parameters was performed on the basis of the selected volume of interest (VOI), to obtain the 3-dimensional interpretation [48] (**Figure 14**). All image processing steps were conducted automatically using Image Processing Language (IPL, Scanco Medical AG, Brüttisellen).

Due to different quantitative threshold values it was possible to detect the bone automatically and separate the callus from the bone without having to draw regions of interest (ROI) [101]. Besides saving time, the advantage of this procedure is that the near impossible separation of the bone caused by too many ROIs within the fracture gap becomes an unnecessary task.

The following measures of bone structure and composition were evaluated from the µ-CT image data for each specimen: Bone volume (BV); tissue mineral density (TMD) = material density = bone tissue density = degree of mineralisation; bone mineral content (BMC), defined as callus BV multiplied by TMD; trabecular thickness (Tb. Th.); degree of anisotropy (DA); bone surface (BS); structure model index (SMI)[63].

Figure 14:

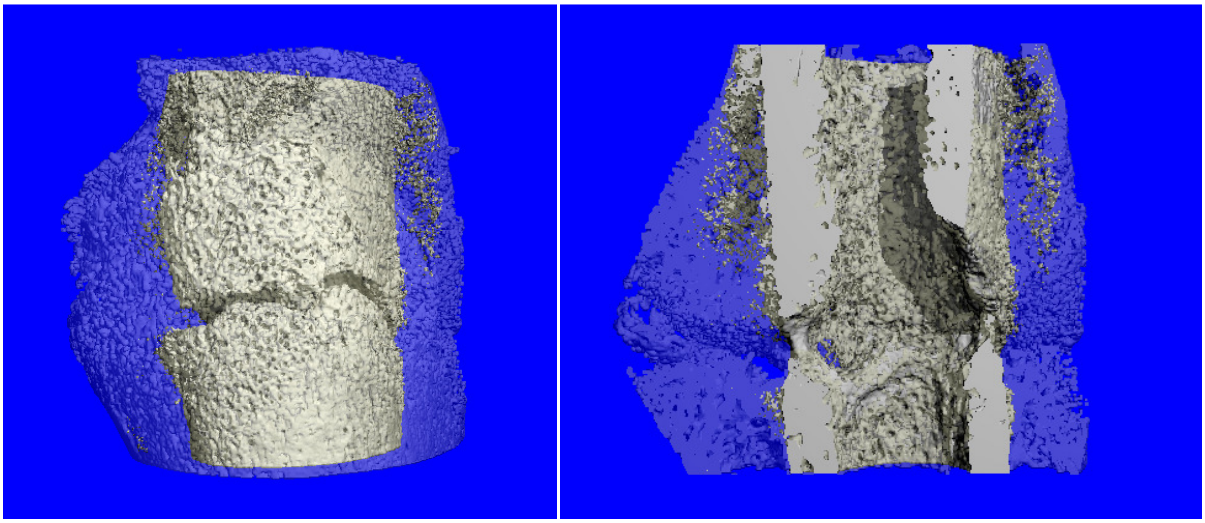

Figure 14: µCT scan, 3-dimensional reconstruction of ROI, virtually sliced in half. 3-D rendering of the entire volume of interest and a corresponding longitudinal cut-away view for a representative specimen

Biomechanical Testing

Biomechanical examination of the specimens was done by three-point bending using a Zwick material testing machine (Zwicki 1120, Zwick GmbH & Co, Ulm, Germany). Positioning for three-point-bending was carried out with force transmission at the evaluated middle position between the distal and the proximal site of each femur (**Figure 15**). Bearing- and loading-bars had a rounded tipp with a diameter of 2.5mm. The distance between the bars was adapted for each bone. The femora (n = 90) were placed on their posterior surface on the lower supports of the bending apparatus. These supports were adjusted individually so that the first support was placed just distal to the trochanter minor and the other support just proximal to the condyles of the femur (popliteal plane) [44]. All bones were loaded until failure (V-max) with a persistent test velocity of 5mm/min. Meanwhile a load-displacement diagram was recorded every 0.1 second and thereby failure load was determined (**Figure 16**). Measurement was done with a load sensor for 2.5 KN (Klasse 0.05, A.S.T. GmbH, Dresden, Germany). The stiffness was defined as linear regression with TestXpert V12 software.

Figure 15:

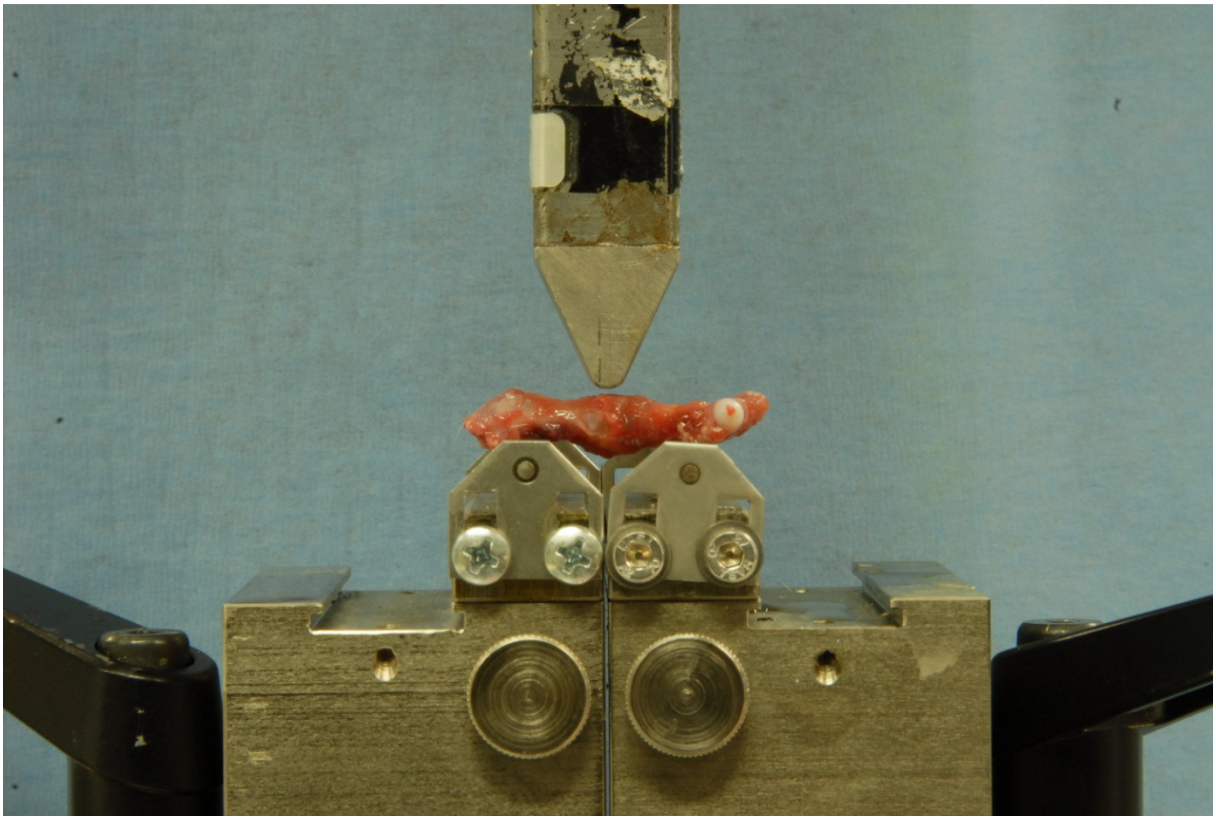

Figure 15: Setting during biomechanical testing of the specimens. The distance between the bars was adapted for each bone individually.

Figure 16:

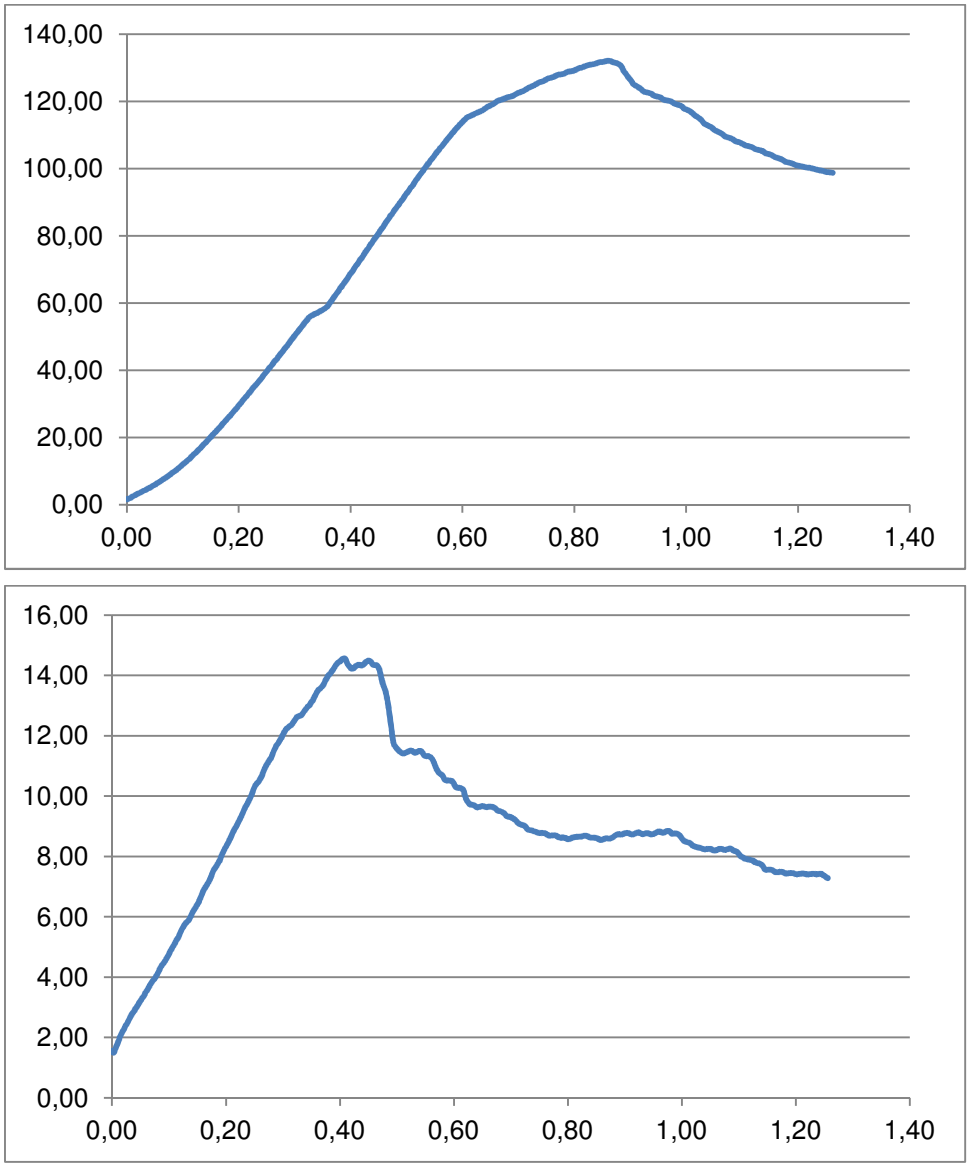

Figure 16: Load-displacement diagram of corresponding bones. In the first picture the fracture-curve of the control side, in the second the experimental side is displayed. The ordinate displays the force (N), the abscisse the displacement (in mm). Note: Different scales of the ordinate.

Sample Size Estimation

Sample size estimation was done according to the specifications by Leppänen et al. regarding biomechanical testing in animal models [58]. By allocating at least 14 animals per group, recognition of expected treatment effects of 10% would be feasible with statistical power of 90% at a significance level of $p<0.05$ in the femur shaft three-point bending test. So the group size for the biomechanical testing was defined with 15 animals per group.

Morphological examinations by Micro-CT were seen as explorative adjunct. Therefore the minimum group size was determined with 6 animals.

Statistical Analysis

Failure load and stiffness were collected for each bone of the biomechanical group. Absolute as well as relative values (failure load and stiffness of the experimental side in relation to the contralateral, healthy bone) were determined. The acquired data were collected in a data base and statistically analyzed by SPSS (Version 21, IBM Statistics). Differences between the groups were calculated by ANOVA (Kruskall-Wallace test). Level of significance was set at $p<0.05$.

Statistical analyses of the micro-CT scans were performed with R 2.15.1 (The R Foundation for Statistical Computing, Vienna, Austria). As the data showed no severe deviations from the normal distribution, descriptive statistics are given by mean ± standard deviation. Accordingly, group comparisons were performed by t-tests. Corresponding mean differences with 95% confidence intervals are presented with p-values. Graphical presentations of the data distribution are given by dot plots and error bars. All tests were two-sided and performed in an explorative manner on a 5% significance level.

VI. Results

In total 70 male Wistar rats (Crl:WI), obtained from Charles River Laboratories, Sandhofer Weg 7, 97633 Sulzfeld, Germany were used. All Rats were 15 weeks old at the time of surgery weighting between 380 and 480 g.

We only lost 2 animals during the experiment (2.9%). Rat 1 was euthanized during surgery due to the fact, that the femoral shaft was accidentally penetrated with the K- wire. Rat 42 developed a subcutaneous hematoma, 1cm x 1cm in size, located above the greater trochanter. As the animal showed pale mucous membranes and a poor general condition, the experiment was terminated and the rat humanely euthanized. This decision was based on the grounds that severe blood loss would jeopardize the comparability of the results, as well as to prevent unnecessary pain and distress for the animal.

Rats 16, 20, 22, 33 and 35 developed a hematoma, located above the greater trochanter, but were in good general condition. All rats that developed hematoma, inclusive rat 42, belonged to the Enoxaparin group. So the prevalence of hematomas in the Enoxaparin group was 37.5% whereas no relevant hematoma could be seen in the Rivaroxaban or in the control-group.

Rats 3, 4 and 5 were excluded after euthanasia, because the originally estimated dosages for Rivaroxaban and Enoxaparin, who later showed to be insufficient, had been used in these rats.
Rat 26 (Rivaroxaban) did not put weight on the operated leg as early as other rats and showed slight lameness starting at day 11 after surgery. Necropsy revealed a fractured femoral neck.
Rat 33 (control) did not put much load on the operated leg and a slight lameness was observed as well. Necroscopy showed an intramuscular seroma above the pin.

All other animals showed good, postoperative conditions, gained weight during the experiment and used their operated leg normally at least 3 days after the surgery.

Biomechanical Testing

A total of 45 animals were investigated by biomechanical testing. After euthanasia both femora were harvested and subject to three-point bending (n=90).
In all 90 femura the failure load could be determined. In 2 bones, both experimental sides (1 in the Rivaroxaban-group, 1 in the Enoxaparin-group) the stiffness could not be calculated due to absence of linear characteristics in the load-displacement diagram.

Failure Loads (V-max)

Failure loads of the experimental sides averaged 24.67 N (+/- 11.85 N) for the controls, 25.28 N (+/- 11.28 N) for Rivaroxaban and 22.88 N (+/- 8.1 N) for Enoxaparin. The contralateral, unfractured bones counted up for 142.1 N (+/- 20.8 N) for the controls, 135.9 N (+/- 20.47 N) for Rivaroxaban and 140.1 N (+/- 17.1 N) for Enoxaparin. Values for every fractured bone, minima and maxima are displayed in **Tables 7 to 10.**

Stiffness

Stiffness was deduced in obtaining the gradient of the linear part of the load-displacement curve. For the experimental sides it was defined as the interval between 2 N and 10 N, for the controls between 20 N and 80 N. Manual corrections were applied if necessary (e.g. short, linear part of the curve; later or earlier onset…)
Stiffness of experimental bones averaged 27.83 N/mm (+/- 22.35 N/mm) for controls, 23.1 N/mm (+/- 14.43 N/mm) for Rivaroxaban and 18.35 N/mm (+/- 7.2 N/mm) for Enoxaparin. The contralateral sides were 230.9 N/mm (+/- 50.48 N/mm) in the control-group, 214.13 N/mm (+/- 48.07 N/mm) in the Rivaroxaban-group and 227.1 N/mm (+/- 29.46 N/mm) for Enoxaparin. Values for every fractured bone, minima and maxima are displayed in **Tables 7 to 10**.

Table 7:

Animal (Nr.)	Group	Side	Vmax (N)	Stiffness (N/mm)
2	control	unfractured	113,06	217,46
2	control	fracture	61,73	91,9
8	control	unfractured	109,8	160,58
8	control	fracture	21,63	18,58
10	control	unfractured	145,87	216,63
10	control	fracture	13,6	5,74
11	control	unfractured	167,23	272,61
11	control	fracture	15,29	14,23
12	control	unfractured	161,11	307,87
12	control	fracture	22,19	15,13
13	control	unfractured	169,73	285,21
13	control	fracture	16,68	9,72
14	control	unfractured	133,89	237,4
14	control	fracture	19,86	33,86
18	control	unfractured	143,34	232,63
18	control	fracture	28,05	20,54
25	control	unfractured	143	240,23
25	control	fracture	16,7	45,21
43	control	unfractured	118,03	197,38
43	control	fracture	21,68	11,64
56	control	unfractured	133,28	258,55
56	control	fracture	26,91	45,71
61	control	unfractured	117,6	113,14
61	control	fracture	16,38	10,78
63	control	unfractured	149,81	252,94
63	control	fracture	29,19	46,42
66	control	unfractured	154,75	195,1
66	control	fracture	25,32	22,22
69	control	unfractured	171,33	276,54
69	control	fracture	34,86	25,78

Table 7: Control-group, biomechanical testing. Single values for every fractured bone (Vmax = Strength = Failure load in Newton, Stiffness (Newton/mm))

Table 8:

Animal (Nr.)	Group	Side	Vmax (N)	Stiffness (N/mm)
15	Rivaroxaban	unfractured	133,87	251,88
15	Rivaroxaban	fracture	12,12	11,6
17	Rivaroxaban	unfractured	133,74	232,91
17	Rivaroxaban	fracture	14,22	10,76
19	Rivaroxaban	unfractured	138,51	233,21
19	Rivaroxaban	fracture	7,3	-
21	Rivaroxaban	unfractured	173,97	262,88
21	Rivaroxaban	fracture	32,3	18,47
23	Rivaroxaban	unfractured	140,34	234,53
23	Rivaroxaban	fracture	22,83	22,31
24	Rivaroxaban	unfractured	130,92	220,15
24	Rivaroxaban	fracture	37,28	22,09
26	Rivaroxaban	unfractured	148,47	205,65
26	Rivaroxaban	fracture	34,9	48,51
28	Rivaroxaban	unfractured	136,04	238,25
28	Rivaroxaban	fracture	30,76	16,92
41	Rivaroxaban	unfractured	118,86	179,55
41	Rivaroxaban	fracture	47,22	49,5
44	Rivaroxaban	unfractured	124,77	195,33
44	Rivaroxaban	fracture	31,11	47,51
48	Rivaroxaban	unfractured	127,92	222,32
48	Rivaroxaban	fracture	17,94	7,8
60	Rivaroxaban	unfractured	131,63	228,84
60	Rivaroxaban	fracture	16,96	18,42
62	Rivaroxaban	unfractured	168,48	261,15
62	Rivaroxaban	fracture	20,98	15,87
62a	Rivaroxaban	unfractured	85,53	68,13
62a	Rivaroxaban	fracture	17,17	12,6
67	Rivaroxaban	unfractured	146,28	177,18
67	Rivaroxaban	fracture	36,14	21,26

Table 8: Rivaroxan-group, biomechanical testing. Single values for every fractured bone (Vmax = Strength = Failure load in Newton, Stiffness (Newton/mm))

Table 9:

Animal (Nr.)	Group	Side	Vmax (N)	Stiffness (N/mm)
16	Enoxaparin	unfractured	149,05	237,18
16	Enoxaparin	fracture	27,13	17,36
20	Enoxaparin	unfractured	133,07	212,95
20	Enoxaparin	fracture	10,9	-
22	Enoxaparin	unfractured	156,63	264,66
22	Enoxaparin	fracture	17,07	12,25
27	Enoxaparin	unfractured	156,85	280,88
27	Enoxaparin	fracture	13,25	14,34
45	Enoxaparin	unfractured	132,34	179,59
45	Enoxaparin	fracture	20,79	26,33
46	Enoxaparin	unfractured	117,07	198,9
46	Enoxaparin	fracture	20,15	23,45
47	Enoxaparin	unfractured	122,6	220,11
47	Enoxaparin	fracture	21,48	14,22
54	Enoxaparin	unfractured	133,13	203,13
54	Enoxaparin	fracture	18,63	13,58
55	Enoxaparin	unfractured	111,89	199,8
55	Enoxaparin	fracture	22,47	11,58
57	Enoxaparin	unfractured	129,71	199,43
57	Enoxaparin	fracture	23,3	15,84
58	Enoxaparin	unfractured	130,56	216,61
58	Enoxaparin	fracture	30,04	21,42
59	Enoxaparin	unfractured	144,9	250,54
59	Enoxaparin	fracture	16,15	8,85
64	Enoxaparin	unfractured	157,93	263,64
64	Enoxaparin	fracture	27,21	23,49
65	Enoxaparin	unfractured	169,74	244,68
65	Enoxaparin	fracture	42,78	35,98
68	Enoxaparin	unfractured	155,83	234,48
68	Enoxaparin	fracture	31,79	18,33

Table 9: Enoxaparin-group, biomechanical testing. Single values for every fractured bone (Vmax = Strength = Failure load in Newton, Stiffness (Newton/mm))

Table 10:

Overview										
Substance		N valid	N missing	Mean	Median	Standard deviation	Minimum	Maximum	Percentile 25	Percentile 75
Vmax unfractured femur (N)	Enoxaparin	15	0	140,1	133,1	17,1	111,9	169,7	129,7	156,6
	Control	15	0	142,1	143,3	20,8	109,8	171,3	118,0	161,1
	Rivaroxaban	15	0	136,0	133,9	20,5	85,5	174,0	127,9	146,3
Vmax fracture (N)	Enoxaparin	15	0	22,9	21,5	8,1	10,9	42,8	17,1	27,2
	Control	15	0	24,7	21,7	11,9	13,6	61,7	16,7	28,1
	Rivaroxaban	15	0	25,3	22,8	11,3	7,3	47,2	17,0	34,9
Stiffness unfractured femur	Enoxaparin	15	0	227,1	220,1	29,5	179,6	280,9	199,8	250,5
	Control	15	0	231,0	237,4	50,5	113,1	307,9	197,4	272,6
	Rivaroxaban	15	0	214,1	228,8	48,1	68,1	262,9	195,3	238,3
Stiffness fracture	Enoxaparin	14	1	18,4	16,6	7,2	8,9	36,0	13,2	23,5
	Control	15	0	27,8	20,5	22,4	5,7	91,9	11,6	45,2
	Rivaroxaban	14	1	23,1	18,4	14,4	7,8	49,5	12,4	28,6
Ratio Vmax	Enoxaparin	15	0	0,2	0,2	0,1	0,1	0,3	0,1	0,2
	Control	15	0	0,2	0,2	0,1	0,1	0,5	0,1	0,2
	Rivaroxaban	15	0	0,2	0,2	0,1	0,1	0,4	0,1	0,2
Ratio Stiffness	Enoxaparin	14	1	0,1	0,1	0,0	0,0	0,1	0,1	0,1
	Control	15	0	0,1	0,1	0,1	0,0	0,4	0,1	0,2
	Rivaroxaban	14	1	0,1	0,1	0,1	0,0	0,3	0,1	0,2

Table 10: Summary, statistical overview. Mean, median and SD of the three tested groups, minima and maxima, percentiles of Vmax (fracture side/unfractured side), stiffness (fracture side/unfractured side) and ratios.

Comparison between the Groups

In general, absolute values, standard deviations of the mean and relative values showed homogenous patterns throughout the groups (**Table 10**).

V-max (failure load) of the control-side was between 136N and 142N in the mean, the experimental side averaged with 22.9N to 25.3N. As expected, stiffness showed a slightly higher variance in both and was calculated with 214 to 231 and 18.4 to 27.8 respectively.

After 21 days the callus of the fractured femur reached between 16 and 19% of the strength (evaluated by obtaining V-max) of the corresponding, contralateral bone.

Comparison of groups did not show differences between the tested substances and controls with a high degree of significance (**Figures 17 – 20, Table 11**).

Figure 17:

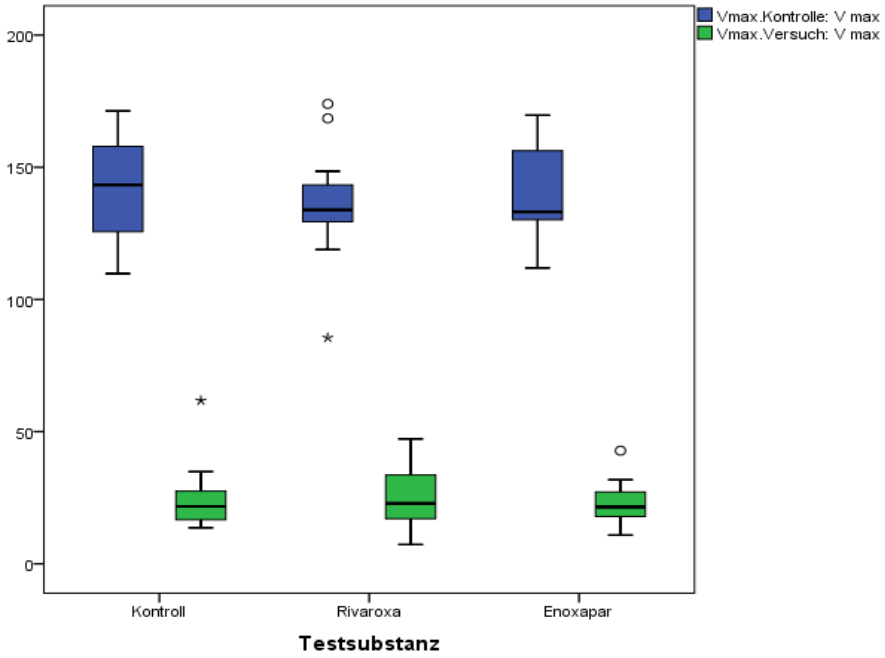

Figure 17: Box-plot of absolute V-max values for controls, Rivaroxaban and Enoxaparin. Blue boxes reveal the contralateral, unfractured bones. Green boxes reveal experimental sides.

Figure 18:

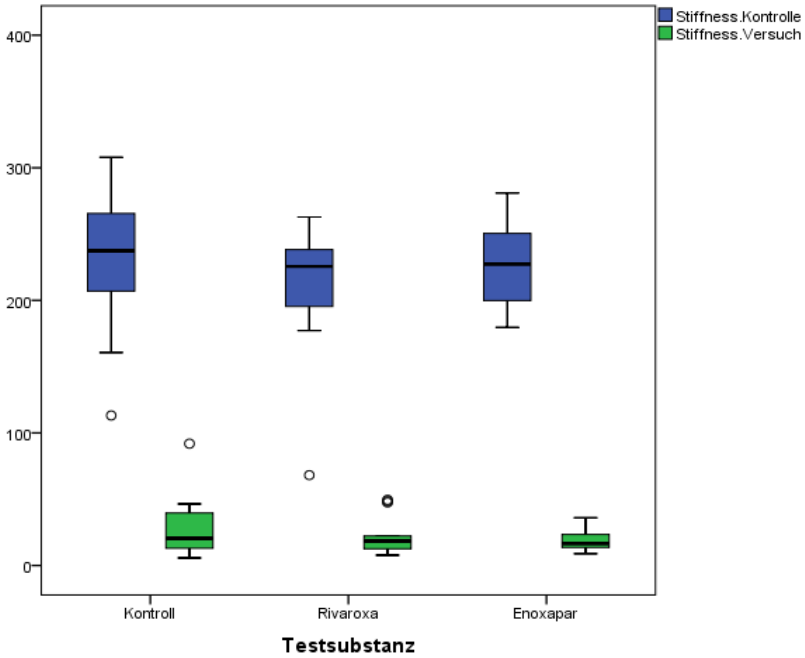

Figure 18: Box-plot of absolute Stiffness values for controls, Rivaroxaban and Enoxaparin. Blue boxes reveal the contralateral, unfractured bones. Green boxes reveal experimental sides.

Figure 19:

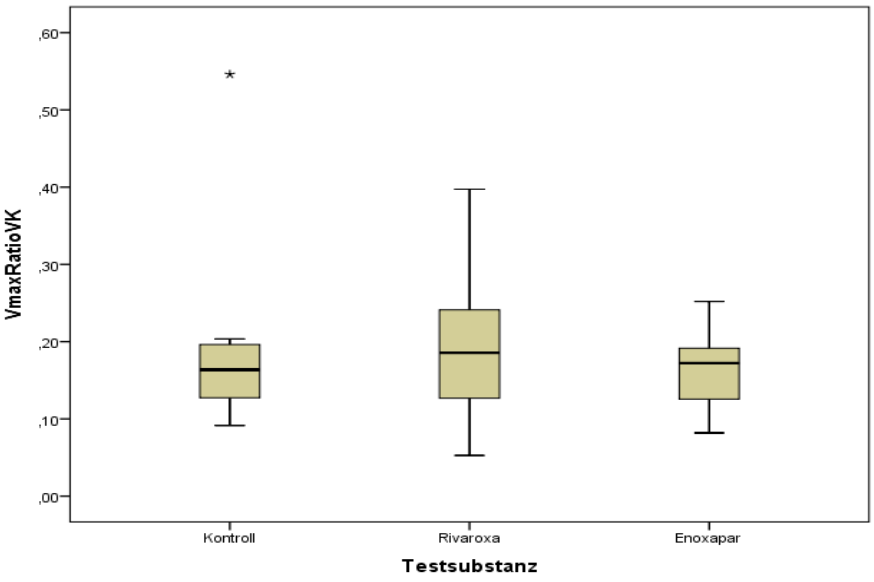

Figure 19: Box-plot of ratios fractu**red to unfractured bones in V-max for controls, Rivaroxaban and Enoxaparin.**

Figure 20:

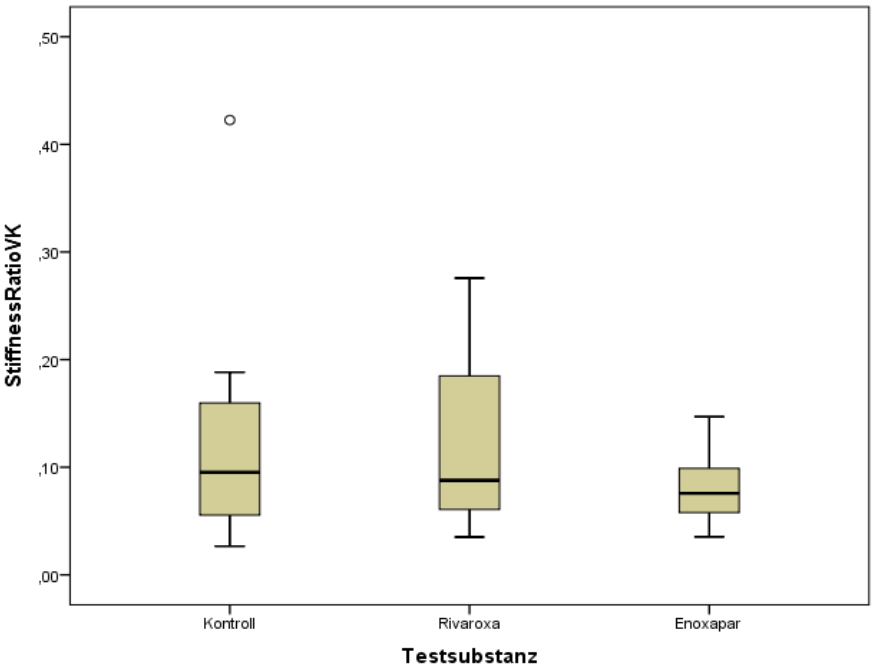

Figure 20: Box-plot ratios fractured to unfractured bones in stiffness for controls, Rivaroxaban and Enoxaparin.

Table 11:

Übersicht über Hypothesentest

	Nullhypothese	Test	Sig.	Entscheidung
1	Die Verteilung von Vmax.Kontrolle: V max ist über Kategorien von Testsubstanz gleich.	Kruskal-Wallis-Test unabhängiger Stichproben	,745	Nullhypothese behalten.
2	Die Verteilung von Vmax.Versuch: V max ist über Kategorien von Testsubstanz gleich.	Kruskal-Wallis-Test unabhängiger Stichproben	,794	Nullhypothese behalten.
3	Die Verteilung von Stiffness. Kontrolle ist über Kategorien von Testsubstanz gleich.	Kruskal-Wallis-Test unabhängiger Stichproben	,605	Nullhypothese behalten.
4	Die Verteilung von Stiffness. Versuch ist über Kategorien von Testsubstanz gleich.	Kruskal-Wallis-Test unabhängiger Stichproben	,721	Nullhypothese behalten.
5	Die Verteilung von VmaxRatioVK ist über Kategorien von Testsubstanz gleich.	Kruskal-Wallis-Test unabhängiger Stichproben	,715	Nullhypothese behalten.
6	Die Verteilung von StiffnessRatioVK ist über Kategorien von Testsubstanz gleich.	Kruskal-Wallis-Test unabhängiger Stichproben	,568	Nullhypothese behalten.

Asymptotische Signifikanzen werden angezeigt. Das Signifikanzniveau ist ,05.

Table 11: Testing of hypothesis: No significant differences between the tested substances and the controls could be found.

Micro CT

The results were illustrated qualitatively by three-dimensional reconstructions of representative specimens (see **Figure 14**) and quantitatively for each experiment. Altogether 20 bones were examined (7 in the Rivaroxaban-, 7 in the Enoxaparin-group, and 6 controls). One control-animal (rat 2) was lost intraoperatively and had to be euthanized.
Absolute values of the obtained parameters are shown in **Table 12**.

Table 12:

Meas.Nr.	Ratte	Gruppe	Therapie	BV	Dichte [mg HA/ccm]	BMC	TRI-SMI	DA	BS	DT-Tb.Th*
2633	FEMUR_53V		Riva	68,654	619,369	42,522	-0,8820	1,1047	1573,85	0,1000
2644	FEMUR_36V		Riva	73,740	644,072	47,494	-0,8734	1,1954	1692,50	0,0992
2646	FEMUR_33V		Kontrolle	58,172	643,189	37,416	-1,2248	1,1540	1272,15	0,1012
2647	FEMUR_38V		Kontrolle	64,275	645,748	41,506	-0,1844	1,1602	1462,63	0,1076
2648	FEMUR_39V		Riva	96,791	642,219	62,161	-0,8449	1,1185	2198,99	0,0995
2649	FEMUR_29V		Kontrolle	64,074	644,408	40,577	-1,0957	1,1672	1277,66	0,1036
2650	FEMUR_37V		Riva	80,191	634,172	50,519	-1,2621	1,1381	1781,93	0,1001
2651	FEMUR_49V		Riva	75,215	619,545	46,599	-1,6773	1,1295	1634,08	0,0991
2652	FEMUR_31V		Kontrolle	63,938	646,933	42,424	-1,0872	1,1830	1432,64	0,1042
2653	FEMUR_50V		Enoxa	84,768	645,130	54,686	-0,8399	1,1102	1967,75	0,0981
2654	FEMUR_06V		Kontrolle	61,263	648,218	39,712	-0,8079	1,1954	1284,23	0,1060
2655	FEMUR_09V		Riva	76,937	637,014	49,010	-1,6097	1,0871	1654,56	0,0994
2656	FEMUR_35V		Enoxa	61,138	646,542	39,528	-0,8292	1,1316	1367,28	0,1013
2657	FEMUR_34V		Enoxa	77,348	638,425	49,381	-1,8012	1,1229	1548,75	0,1079
2662	FEMUR_51V		Riva	92,640	652,100	60,410	-1,7711	1,1556	1966,61	0,1008
2663	FEMUR_05V		Enoxa	85,879	649,277	55,759	-1,5581	1,1730	1838,56	0,1008
2664	FEMUR_30V		Enoxa	60,776	633,838	38,522	-0,1569	1,1332	1431,43	0,1008
2672	FEMUR_52V		Kontrolle	70,688	646,542	45,703	-2,1655	1,1780	1432,79	0,1029
2673	FEMUR_40V		Enoxa	67,180	635,426	42,688	-0,8741	1,1184	1516,69	0,1005
2674	FEMUR_32V		Enoxa	61,932	624,221	38,659	-0,1278	1,1617	1498,76	0,0986

Table 12: Absolute values of micro-CT parameters for each animal (bone). Displayed are bone volume (mineralized callus volume = BV), density of the callus (tissue mineral density TMD = Dichte), bone mineral content BMC (defined as the callus BV multiplied by TMD), the structure model index (SMI), the degree of anisotropy DA, trabecular thickness (Tb-Th) and the bone-surface (BS).

The quantification of bone volume (mineralized callus volume = BV) in the fractured femoral diaphysis is shown in **Figure 21**. The Rivaroxaban- as well as the Enoxaparin-group had higher callus volume than the control group. A statistically significant difference between the Rivaroxaban-group and the control group was measured (p = 0,004).

Figure 21:

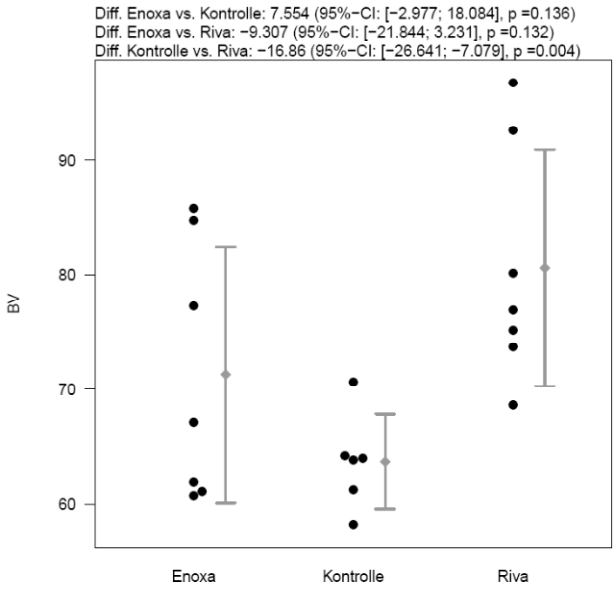

Figure 21: Micro-CT based assessment of histomorphometry by measuring the bone volume BV (mm^3) = mineralized callus volume; Enoxa(parin), Kontrolle = control group; Riva(roxaban), black point indicates exact data, grey arbor mean data ± standard deviation; above difference of each group (95% confidence interval); significant difference of Riva compared to control group (p = 0,004)

The density of the callus (tissue mineral density TMD) was lower in both groups treated either with Rivaroxaban or Enoxaparin compared to the control group (see **Figure 22**). No significant difference could be obtained. The bone mineral content BMC (defined as the callus BV multiplied by TMD) showed corresponding to BV a higher score in the treated rats. The Rivaroxaban-group showed again a statistically higher BMC than the control group (p = 0.01) (**Figure 23**).

The structure model index (SMI) quantifies the plate and rod characteristic of 3D-trabecular-structure [40]. SMI is negative in case of concave surfaces, like in trabecular bone. The SMI in our investigation did not show significant changes between the groups (**Figure 24**). The degree of anisotropy DA as well as the trabecular thickness (Tb-Th) showed statistically significant lower results in the treated groups compared to the control group (see **Figures 25 and 26**). Bone surface (BS) is determined by triangulating the surface and calculating the total area of triangles. The surface of the bone (BS) was found significant higher in the Rivaroxaban- (p = 0,002) and the Enoxaparin-group (p = 0,033) than the BS in the control group (see **Figure 27**). Reflecting all histomorphometric measures, no statistically significant difference could be seen between Rivaroxaban and Enoxaparin. Their alterations seemed to be equally sensed compared to the results obtained from the control group.

Figure 22:

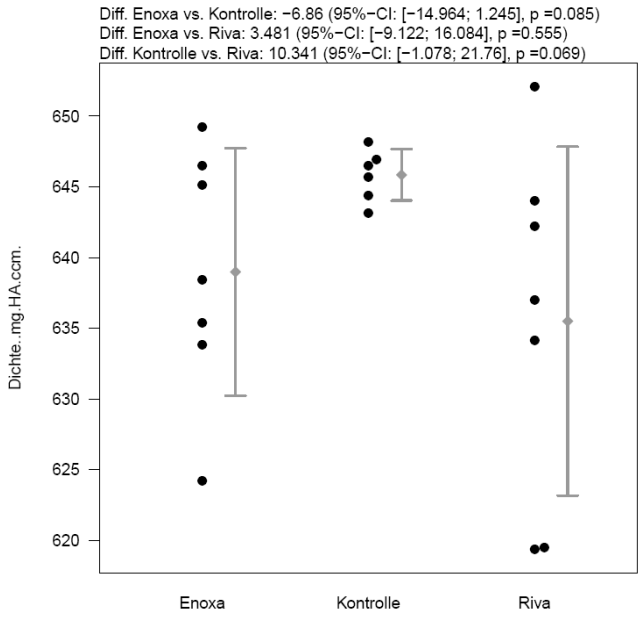

Figure 22: Micro CT based assessment of histomorphometry by measuring the tissue mineral density = Dichte (mg hydroxyapatit/ ccm); Enoxa(parin), Kontrolle = control group; Riva(roxaban) black point indicates exact data, grey arbor mean data ± standard deviation; above difference of each group (95% confidence interval); no significant difference compared to control group (p < 0,05).

Figure 23:

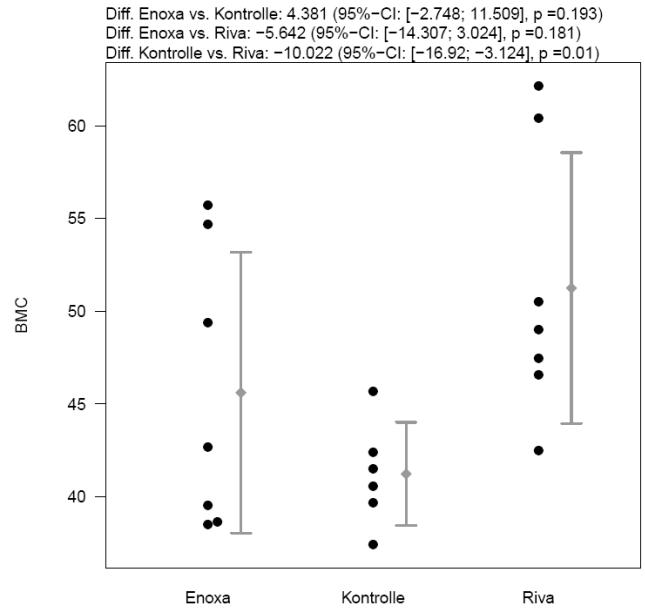

Figure 23: Micro CT based assessment of histomorphometry by measuring the bone mineral content = BMC defined as callus BV multiplied by TMD (mg hydroxyapatit/ ccm) ; Enoxa(parin), Kontrolle = control group; Riva(roxaban) black point indicates exact data, grey arbor mean data ± standard deviation; above difference of each group (95% confidence interval); significant difference of Riva compared to control group (p < 0,05).

Figure 24:

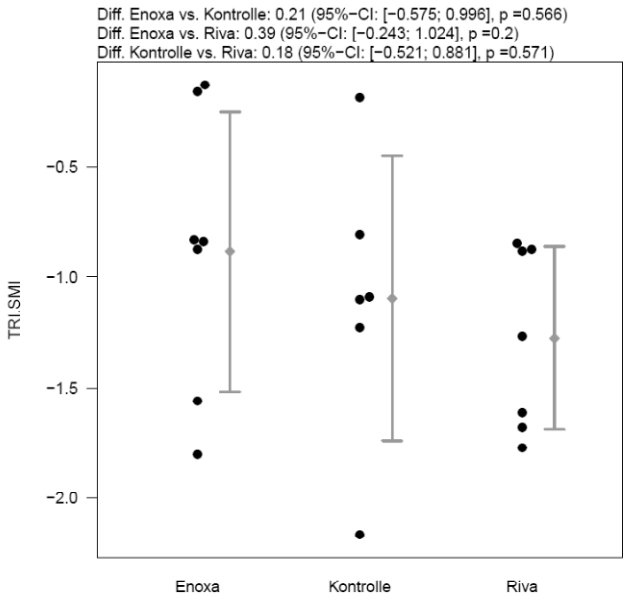

Figure 24: Micro-CT based assessment of histomorphometry by measuring the structure model index = SMI; Enoxa(parin), Kontrolle = control group; Riva(roxaban) black point indicates exact data, grey arbor mean data ± standard deviation; above difference of each group (95% confidence interval); no significant difference compared to control group (p = 0,01).

Figure 25:

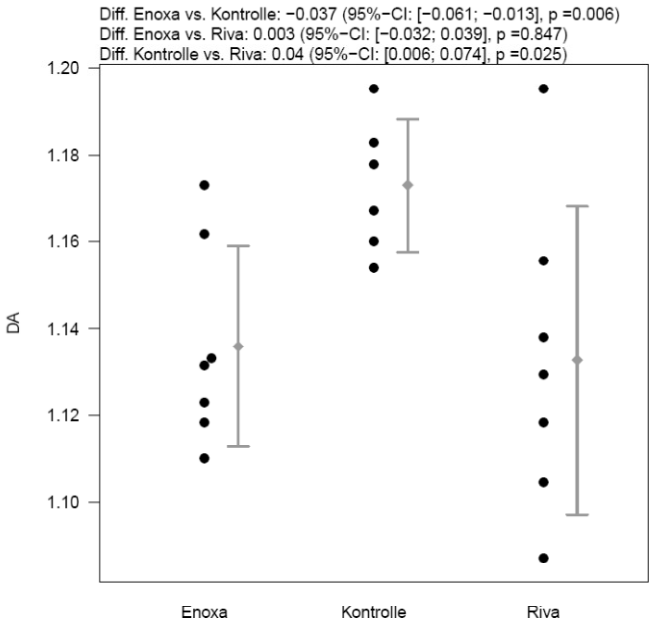

Figure 25: Micro-CT based assessment of histomorphometry by measuring the degree of anisotropy = DA; Enoxa(parin), Kontrolle = control group; Riva(roxaban) black point indicates exact data, grey arbor mean data ± standard deviation; above difference of each group (95% confidence interval); significant difference compared to control group (p < 0,05).

Figure 26:

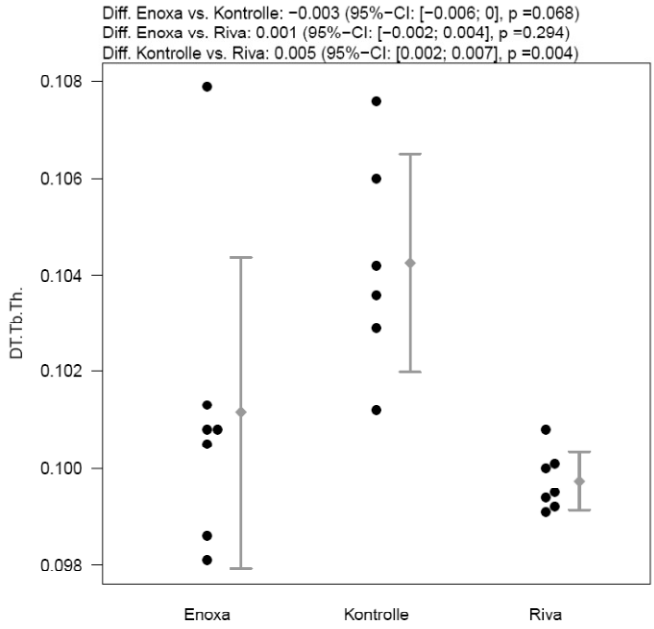

Figure 26: Legend: Micro-CT based assessment of histomorphometry by measuring the trabecular thickness = Tb-Th (mm); Enoxa(parin), Kontrolle = control group; Riva(roxaban) black point indicates exact data, grey arbor mean data ± standard deviation; above difference of each group (95% confidence interval); significant difference of Riva compared to control group (p < 0,05).

Figure 27:

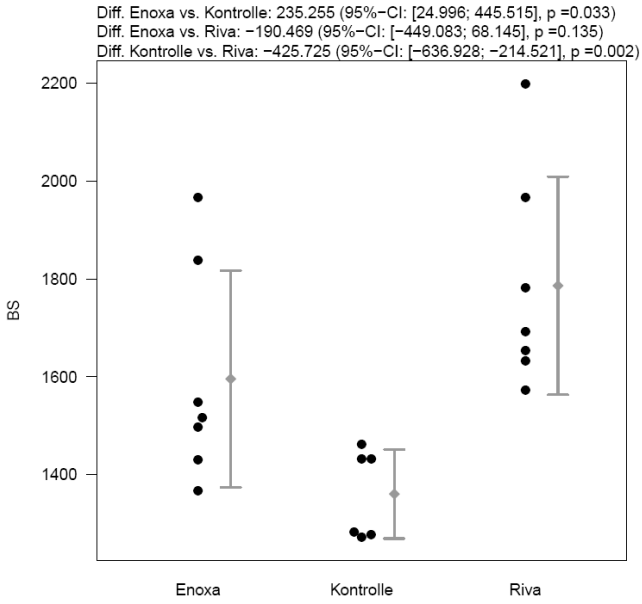

Figure 27: Micro-CT based assessment of histomorphometry by measuring the bone surface = BS (mm²); Enoxa(parin), Kontrolle = control group; Riva(roxaban) black point indicates exact data, grey arbor mean data ± standard deviation; above difference of each group (95% confidence interval); significant difference compared to control group (p < 0,05).

Summary of Biomechanical and Histomorphometric Examinations

Table 13:

	Failure Load	Stiffness	Bone Volume	Density	Bone Mineral Content	Structure Model Index	Degree of Anisotropy	Bone Surface	Trabecular Thickness
Rivaroxaban	-	-	↑↑	↓	↑↑	-	↓↓	↑↑	↓↓
Enoxaparin	-	-	↑	↓	↑	-	↓↓	↑↑	↓

Table 13: Summary of Results in comparison to control-group: - = equal; ↑ = enhanced, ↑↑ = significantly enhanced; ↓ = reduced, ↓↓ = significantly reduced

VII. Discussion

Long term administration of heparin and LMWH has been associated with negative effects on bone and increased risk of developing osteoporosis during pregnancy [10, 69, 81, 99]. As orthopedic patients are frequently subject to long-term anticoagulation via LMWH in order to prevent thromboembolic events, it has been questioned whether this treatment would negatively interfere with bone healing. Street et al. found a significant delay in fracture healing in an unstabilized rabbit rib fracture model following the administration of Enoxaparin [94]. In his study, fracture healing was investigated by histology, histomorphometry, and immunohistochemistry at days 3, 7, and 14, and by mechanical testing after 21 days following fracture. At days 3, 7, and 14, fewer proliferating cells and fewer transforming pericytes in the medullary callus of the Enoxaparin-treated rabbits were found. In the Enoxaparin group, the grade of fracture healing was reduced at days 7 and 14, and the mechanical properties were weaker at day 21 compared to controls. In contrast, Hak et al. investigated Dalteparin in a standard stabilized rat femur fracture model and were not able to observe any deleterious effects [35]. Animals were sacrificed at 2, 3, and 6 weeks and fracture healing was assessed by radiographs, histology, and mechanical testing. There were no significant differences between the control and LMWH groups in the percentage of animals with radiographic bridging callus at each time point. Histologic appearance of fracture healing was similar between the control and LMWH groups and there were no significant differences in the normalized mechanical properties of the control and LMWH groups at 2 and 3 weeks, with even showing increased torsional strength for LMWH at 6 weeks.

Variable effects on bone have been shown with distinct formulations of LMWHs. Fondaparinux for example was shown to cause higher mitochondrial activity and protein synthesis in osteoblasts compared to Enoxaparin and unfractionated heparin [61].
Negative effects tend to increase with experimental overdoses. In an in vitro bone nodule assay, supertherapeutic doses of LMWH have been proven to decrease cancellous bone volume, demonstrated by a lack of normal remodeling and repair [5]. Supertherapeutic doses also produced a decrease in the osteoid surface area and alkaline phosphatase activity in a dose-dependent manner [65].

The mechanism of how anticoagulant medication interferes with bone-healing is still not clear. Obviously there might be some effect on the fracture-hematoma which plays a crucial role in the restoration of fractured bones. With routine use of LMWH in total hip arthroplasty a higher rate of surgical side hematomas has been reported [25]. Thus, the early use of LMWH in orthopedic patients suffering fractures may presumably lead to larger fracture site hematoma.

As Mizuno et al. stated the osteogenic potential of the fracture side hematoma, its significance and beneficial role has been generally accepted [62]. Several studies have shown that evacuation of this hematoma can be deleterious, especially when performed several days following fracture, after the inflammatory phase has ended [34, 72]. In contrast, Street et al. observed that the high potassium (K^+) concentration of fracture site hematoma is cytotoxic to endothelial cells and osteoblasts and therefore inhibits bone formation [93]. Only after these cytotoxic elements have undergone resporption, the angiogenic and osteogenic cytokines present in fracture hematoma come to function. Brighton and Hunt described an area of architectural disruption and cell degradation that diminishes with the distance from the hematoma [7]. So increased fracture site hematoma volume as well as lacking hematoma may therefore provide deleterious effects on the physiological cascade of fracture healing.

Unfractioned heparin and in parts LMWH have been shown to provide direct, cell-mediated effects on bone formation and resorption by interfering with osteoblast- and osteoclast-function.

For heparin, negative impact on bone formation by promoting the activation of osteoclasts and decreasing bone volume in rats has been found [11, 64]. This was further specified in vitro and could be linked to enhanced osteoclastic bone resorption through inhibition of osteoprotegerin activity [41] and induction of bone resorption in rat osteoclasts [11, 64]. Furthermore, previous studies have shown that heparin and LMWH, for example Enoxaparin, exert negative effects on alkaline phosphatase expression, as key-protein indicative for osteoblastic function [5, 71]. Ultimately, heparin seems to be able to inhibit BMP-2 osteogenic activity by binding to BMP-2 and the BMP receptor. This effect comes along with reduced Runx2, osteocalcin and alkaline phosphatase expression [46].

There is some evidence that the effects of heparin and its derivatives on osteoblast differentiation are molecular-weight dependent and increase with the molecule-mass. Handschin et al. compared the effects of Dalteparin and Fondaparinux using primary human osteoblasts. Within, Dalteparin was found to produce a significant reduction in osteoblast differentiation and proliferation at a dose of 300µg/ml causing a decline in osteoblast specific

markers, osteocalcin and alkaline phosphatase. In contrast, Fondaparinux, resembling the smaller molecule, did not produce a significant reduction in any of these variables [36]. The critical mass to affect either osteoblast differentiation or mineralization was supposed to be around 3000 Da [5, 71].

Part of the bigger impact of heparin compared to LMWH is the diverse potential to interfere with osteoclast-linages. Muir et al. for example compared the effects of the LMWH (Tinzaparin 0.5–1.0 U/g), with that of heparin (0.5 and 1.0 U/g) in Sprague–Dawley rats and found a dose-dependent decrease in cancellous bone volume for Tinazaparin and unfractioned heparine, which was dramatically higher in heparine [65]. These results were explained by the fact that while both - heparin and LMWH - decreased osteoblast number and activity, only heparin was found to increase the number and activity of osteoclasts. The observation that heparin increases bone resorption while LMWHs do not, is supported by ex vivo studies measuring the release of 45Ca from prelabeled fetal rat calvarias [86]. In this study Shaughnessy et al. were able to show that LMWHs did not stimulate osteoclast activity at concentrations which fall within their therapeutic range and that the concentration of various LMWH (Enoxaparin, Logiparin, Fragmin and Arderparin) had to be increased 50-fold to produce the same effect as unfractioned heparin. Furthermore, no appreciable differences were seen comparing the 4 LMWHs used one to another. To summarize LMWH still cause bone loss, though to notably lesser extent than unfractioned heparin because of the lacking ability to enhance bone resorption.

The reversibility of heparin´s effect on bone was studied by Shaughnessy et al. using a Sprague-Dawley rat model [85]. In this survey rats were treated with 1 U/g/day of heparin for a period of 28 days at which point half the rats were sacrificed. The remaining rats were kept off treatment for an additional 28 days before being sacrificed. Histomorphometric analysis revealed 30% loss in cancellous bone, accompanied by 60% decrease in osteoblast surface and a 137% increase in osteoclast surface in the first group. Importantly, analysis of the second group produced identical results, indicating that the effects of heparin on bone are not readily reversible. With a second experiment using 125I-labeled heparin, the accumulation of heparin in bone and the retention for an extended period of time could be demonstrated. Collectively, these results indicate that heparin's effects on bone are not readily reversible because it remains sequestered within the bone´s microenvironment.

Recently a new, direct factor Xa inhibitor (Rivaroxaban, Xarelto) is available for the prevention of venous thromboembolism in adult patients undergoing elective hip and knee replacement surgery. It has been proven to be highly effective in preventing thromboembolic events [23-24, 33, 54-55, 97]. Coupled with the fact that Rivaroxaban is available orally and eliminating the need for invasive administration, Rivaroxaban is an attractive option for orthopaedic surgeons and patients alike. Regarding the efficacy of the substance, the risk of symptomatic venous thromboembolism in elective joint-replacement surgery was lowered with Rivaroxaban, but considerations of increasing the relative risk of clinically relevant bleeding with this treatment have been drawn [33].

Concerning possible interactions of Rivaroxaban with bone-formation, the actual literature is sparse. Solayer et al. treated primary human osteoblast cultures in vitro with varying concentrations of Rivaroxaban and Enoxaparin and found a significant reduction in osteoblast function for both substances, measured by a decrease in alkaline phosphatase activity. This reduction was associated with reduced mRNA expression of the bone marker osteocalcin, the transcription factor Runx2, and the osteogenic factor BMP-2. Though both agents did not adversely affect osteoblast viability, the authors concluded that Rivaroxaban and Enoxaparin may negatively affect bone through a reduction in osteoblast function, with Rivaroxaban having the major impact [89].
Similarly Gigi et al. observed a dose-dependent inhibition of the DNA-synthesis and creatine kinase-specific activity of SaOS2 cells via Rivaroxaban. In this experiment, SaOS2 cells were treated for 24 hours with different concentrations of Rivaroxaban (0.01-50 µg/ml) and analyzed for DNA synthesis and creatine kinase- and alkaline phosphatase-specific activities. For analyzing mineralization, the treatment was extended 21 days. Rivaroxaban dose-dependently inhibited up to 60% DNA synthesis of the cells. Creatine kinase-specific activity was also inhibited dose-dependently to a similar extent by the same concentrations. Alkaline phosphatase-specific activity was dose-dependently inhibited but only up to 30%. Cell mineralization was unaffected by 10 µg/ml Rivaroxaban. The in vitro model demonstrated a significant Rivaroxaban-induced reduction in osteoblastic cell growth and energy metabolism and slight inhibition of the osteoblastic marker, alkaline phosphatase, while osteoblastic mineralization was unaffected. To summarize, the findings might indicate that Rivaroxaban inhibits the first stage of bone formation [31].

In the given experiment we investigated the influence of Enoxaparin and Rivaroxaban on the biomechanical and morphological properties of new-formed callus in a standardized rodent fracture model.

The results clearly indicate two major conclusions:

- First, the biomechanical characteristics were not altered by the chosen, anticoagulant medication.
- Second, both pharmacons lead to morphological changes of the fracture-callus, more precise to an enhanced callus volume (significant for Rivaroxaban) with reduced density (trend for both substances), to a bigger bone surface (significant for both substances) and in case of Rivaroxaban to significant higher bone mineral content. Furthermore, geometrical parameters as degree of anisotropy and trabecular thickness (only Rivaroxaban significant) were different to controls.

Interpretation and conjunction of these facts is all but trivial.
Several studies have used µ-CT to measure quantities such as bone volume, bone volume fraction, and mineral density in fractured callus [21, 27, 29-30, 84, 87]. However, contradictory results have been reported regarding how well these quantities predict callus mechanical properties or how these values indicate impairment of bone-healing [27, 30, 88].
Higher callus-volume has been previously associated with impaired fracture healing. Shuid et al. studied the effects of calcium supplementation on the late phase healing of fractured, osteoporotic bones using an ovariectomized rat model and were able to demonstrate higher callus volumes after eight weeks in the ovariectomized group compared to controls. Though no clear correlation to biomechanical testing (bending stress and Young's modulus) could be found, the authors concluded that bigger callus could indicate impaired fracture healing of osteoporotic bone due to delay in callus maturation [88]. Contradictory, Morgan et al. correlated larger amounts of callus and tissue mineral density (TMD) positively with better fracture healing [63]. In their survey, the process of fracture healing was strongly linked to an increase in tissue mineral density (TMD) at every investigated time point, whereas absolute and relative amounts of mineralized tissue (BV, BMC) varied. Their results indicate that while the regain of bone strength and stiffness over time is largely due to a time-dependent increase in mineral density, this relationship between mechanical properties and mineral density can be modulated by factors that alter geometry.
TMD seems to represent one of the most important predictors of fracture healing and is strongly correlated to callus mechanical properties. Nyman et al. investigated fracture healing under anabolic treatment in a rat femur fracture model and were able to show that mineralized callus volume inversely and TMD of the callus positively correlated with peak

force as determined by three-point bending, though the correlations were relatively weak [70]. The same behaviour could be demonstrated in an investigation by Hao et al. [37]. The authors confirmed a significantly reduced mineralized bone volume in Micro-CT analysis in osteoporotic rat fractures which implied a delay in fracture healing with decrease of the degree of mineralization.

Similarly to studies investigating insufficient or complicated fracture healing under various circumstances [37, 63, 88] the tested types of anticoagulation, Rivaroxaban as well as Enoxaparin, showed concordant alterations of the new-formed callus, namely and in first rank to enhanced callus volume (BV) with reduced density (TMD) and to a bigger bone surface (BS). This might possibly indicate that both substances – to presume anticoagulation in general – have the potential to interfere with normal bone healing. Causally this could be linked to the hypothetically bigger fracture-hematoma under anticoagulant medication [7, 35, 93] as well as to possible, direct impairment of osteoblasts [5, 31, 71, 89].
To summarize, a bigger and somehow unordered callus was present in both types of medication that ultimately reached the same, biomechanical strength than the untreated controls. In consequence the significance of observable morphological alterations of the callus remains unclear.

Approved human dosages for Enoxaparin are given between 0.6mg/kg (prophylaxis of thrombosis in elective surgery) to 2mg/kg (therapeutical dosage) bodyweight per day. This corresponds to 60 – 200 IU/kg per day. Extrapolations of the human dosages have been used in prior animal studies, Street et al. administered 1mg/kg Enoxaparin per day in a closed rib fracture model in rabbits and were able to prove impairment of fracture-healing [94]. Hak et al. used 70 IU/kg of dalteparin, which represents a similar LMWH in application and indication (prophylactic dose in elective orthopedic surgery would be 5000 IU/day, conform to 70 IU/kg in humans), in a closed rat femur fracture model and observed no differences to his controls [35]. According to experimental experience, a four- to five-fold overdose of human medication is needed in rat models to achieve similar therapeutic results. So we adjusted our first experimental dose of Enoxaparin with 250 IU/kg per day.
Rivaroxaban is administered orally with 10mg (prophylaxis) to 30mg (therapy) per day, which counts up for 0.14mg/kg to approximately 0.42mg/kg bodyweight per day. In the experimental situation the animals were administered orally via enriched feed, which means that a nearly continuous uptake of the pharmacon takes place and that the calculation based on the human application is not adequate. Therefore we referred to the experimental

experience of Bayer Healthcare AG and initiated our pilot study with feed enriched with 1000 ppm of Rivaroxaban.
Rivaroxaban reveals a molecule of the oxazolidinone-group, showing poor hydro-solubility and a 95% to 98% plasmatic binding to albumin. Hence, determination of plasma levels is difficult and of low significance [56, 75-76, 83]. As a result we tempted to equilibrate the two test-groups in the main experiment via adjusting a constant factor Xa-inhibition of 80%. This goal was finally achieved by injecting 1000 IU/kg bodyweight Enoxaparin twice daily on the one- and by application of Rivaroxaban feed containing 600 ppm on the other hand. Concerning the human dosage, this means a 20-fold overdose in the experimental situation.

After 21 days the mechanical strength of the new-formed callus of the right femur reached close to 20% of the strength of the contralateral bone in 3-point bending. The significance of this result is difficult to obtain due to sparse, preexisting literature. Closest to our model comes the work of Hak et al., who tested Enoxaparin-treated femora via torsional testing after 2 and 3 weeks and obtained values between 20% and 35% of the torsional strength in accordance to the contralateral side [35]. Kaspar et al. tested two femora in a standardized rat femur-osteotomy model after two weeks, as well via torsional testing, and found percentage-torques of 9.8% and 13.8% of the contralateral bone [47]. Keeping in mind that torsional testing in general produces higher absolute values and reveals higher variance than 3-point bending, our results are well in line with prior knowledge [43, 58, 96].

Limitations

With 21 days from the fracture to euthanasia, the treatment- or healing-interval of the transverse femur fracture remained relatively short. This was driven by the thought that possible alterations of the fracture-healing process might be linked with the evolution of the fracture-hematoma and should therefore predominantly interfere with the first phase of bone-healing. As resembling a transient state in the physiological process, the effect might thus be transitory and is likely to be compensated later on, especially in animals. Additionally, the *in vitro* experiment by Gigi et al. was indicative that Rivaroxaban inhibits predominantly the first stage of bone formation [31].
Having the experiment terminated after 21 days, it is obviously impossible to determine if and when measurable treatment effects adapt to untreated controls.
Finally, there is no evidence that our standard rat femur fracture model offers any applicability to human fracture healing.

Outlook

Though both anticoagulant substances, Enoxaparin and Rivaroxaban, altered histomorphometric parameters of the new-formed callus, the impact on the biomechanical properties representing the primary endpoint of the study was negligible. Thus clinically relevant delay or impairment of fracture healing must not be expected in general.

Still, there might be certain circumstances in which those effects reach clinical significance. Patients suffering delayed fracture healing or non-union could experience additional disadvantage by long-term administration of anticoagulant medication. In sense of a two- or three-hit mechanism, harmful impacts could act together to finally render restoration of a fractured bone impossible.

In the clinical situation concerns should be made, of how appropriate long-term anticoagulation actually is. Basically, the risk of developing fatal pulmonary thromboembolism has to be balanced against potentially suffering non-union.

More basic research has to be done to explore the pathomechanical pathways of how these drugs act. Finally there seems to be lack of knowledge concerning the cross-linking of hemostatsis and bone healing.

VIII. Summary

Low molecular weight heparine (LMWH) is routinely used to prevent thromboembolism in orthopaedic surgery, especially in the treatment of fractures or after joint-replacement. Impairment of fracture-healing due to increased bone-desorption, delayed remodelling and lower calcification caused by direct osteoclast stimulation is well known for unfractioned heparine, the effect of LMWH is not sure and controversial. Although recent studies did not find any effect, there are others, that strongly suggest impairment *in-vitro* and in the animal model, both characterized by a significant decrease in volume and quality of new-formed callus.

Since October 2008 Rivaroxaban (Xarelto) is available for prophylactic use in elective knee- and hip-arthroplasty. Recently some evidence has been found indicating a dose independent reduction in osteoblast function for this substance *in vitro.*

In this survey, the possible influence of Rivaroxaban and Enoxaparin on bone-healing *in vivo* was studied using a standardized, closed rodent fracture-model. 70 male Wistar-rats were randomized to Rivaroxaban, Enoxaparin or controls. After pinning of the right femur, a closed transverse fracture was produced. 21 days later, the animals were euthanized and both femora harvested. Analysis was done by biomechanical testing (three-point bending) and micro CT.

Both investigated substances showed histomorphometric alterations of the new formed callus assessed by micro CT analysis. In detail the bone (callus) volume was enhanced (sign. for Rivaroxaban) and the density reduced. The bone mineral content was reduced accordingly (sign. for Rivaroxaban). Furthermore both drugs showed significant enlarged bone (callus) surface and trabecular degree of anisotropy. In contrast, the biomechanical properties of the treated bones were equal to controls.

To summarize, the morphological alterations of the fracture-callus did not result in functionally relevant deficits. In the clinical setting, anticoagulant medication might impair fracture healing in delayed- or non-union.

IX. Acknowledgements

I would like to thank my colleagues, forming the joined venture study group “Bone Healing”, a collaboration of the Orthopedic and Maxillofacial Surgery Department of the Technical University of Munich. Especially Kilian Kreutzer, Olliver Bissinger and Franzl Liska should be rewarded for their long nights, assisting me pinning some femurs.

Martina Knödler and Gabriele Wexel, my veterinarians, did a good job in everything that favored the experiments.

Rainer Burgkart, my second doctor-father, should be thanked for his patients and advice.

Tibor Schuster and Alexander Hapfelmeier provided statistical guidance, Eduardo Grande Garcia taught me, how to do biomechanical workup. Thanks for that.

Thomas Tischer and Stephan Vogt should be thanked for bringing me into research.

Bayer Healthcare partially funded the project, especially Dr. von der Osten and Dr. Perzborn were very important to finally conduct the study.

At last, Tinalein was of great importance, of course…

X. References

1. Abu EO, Horner A, Kusec V, Triffitt JT, Compston JE. The localization of the functional glucocorticoid receptor alpha in human bone. *J Clin Endocrinol Metab.* 2000;85:883-889.
2. Aslan M, Simsek G, Yildirim U. Effects of short-term treatment with systemic prednisone on bone healing: an experimental study in rats. *Dent Traumatol.* 2005;21:222-225.
3. Augat P, Margevicius K, Simon J, Wolf S, Suger G, Claes L. Local tissue properties in bone healing: influence of size and stability of the osteotomy gap. *J Orthop Res.* 1998;16:475-481.
4. Barbier A, Martel C, de Vernejoul MC, Tirode F, Nys M, Mocaer G, Morieux C, Murakami H, Lacheretz F. The visualization and evaluation of bone architecture in the rat using three-dimensional X-ray microcomputed tomography. *J Bone Miner Metab.* 1999;17:37-44.
5. Bhandari M, Hirsh J, Weitz JI, Young E, Venner TJ, Shaughnessy SG. The effects of standard and low molecular weight heparin on bone nodule formation in vitro. *Thromb Haemost.* 1998;80:413-417.
6. Bonnarens F, Einhorn TA. Production of a standard closed fracture in laboratory animal bone. *J Orthop Res.* 1984;2:97-101.
7. Brighton CT, Hunt RM. Early histological and ultrastructural changes in medullary fracture callus. *J Bone Joint Surg Am.* 1991;73:832-847.
8. Burchardt H, Glowczewskie FP, Jr., Enneking WF. The effect of Adriamycin and methotrexate on the repair of segmental cortical autografts in dogs. *J Bone Joint Surg Am.* 1983;65:103-108.
9. Burghardt AJ, Kazakia GJ, Laib A, Majumdar S. Quantitative assessment of bone tissue mineralization with polychromatic micro-computed tomography. *Calcif Tissue Int.* 2008;83:129-138.
10. Casele HL, Laifer SA. Prospective evaluation of bone density in pregnant women receiving the low molecular weight heparin enoxaparin sodium. *J Matern Fetal Med.* 2000;9:122-125.
11. Chowdhury MH, Hamada C, Dempster DW. Effects of heparin on osteoclast activity. *J Bone Miner Res.* 1992;7:771-777.
12. Claes LE, Wilke HJ, Augat P, Rubenacker S, Margevicius KJ. Effect of dynamization on gap healing of diaphyseal fractures under external fixation. *Clin Biomech (Bristol, Avon).* 1995;10:227-234.
13. Colwell CW, Jr. Rationale for thromboprophylaxis in lower joint arthroplasty. *Am J Orthop (Belle Mead NJ).* 2007;36:11-13.
14. Cruess RL, Dumont J. Fracture healing. *Can J Surg.* 1975;18:403-413.

15. Dahlman TC. Osteoporotic fractures and the recurrence of thromboembolism during pregnancy and the puerperium in 184 women undergoing thromboprophylaxis with heparin. *Am J Obstet Gynecol.* 1993;168:1265-1270.
16. Day SM, DeHeer DH. Reversal of the detrimental effects of chronic protein malnutrition on long bone fracture healing. *J Orthop Trauma.* 2001;15:47-53.
17. Deguchi M, Rapoff AJ, Zdeblick TA. Posterolateral fusion for isthmic spondylolisthesis in adults: analysis of fusion rate and clinical results. *J Spinal Disord.* 1998;11:459-464.
18. Dekel S, Lenthall G, Francis MJ. Release of prostaglandins from bone and muscle after tibial fracture. An experimental study in rabbits. *J Bone Joint Surg Br.* 1981;63-B:185-189.
19. Dimitriou R, Tsiridis E, Giannoudis PV. Current concepts of molecular aspects of bone healing. *Injury.* 2005;36:1392-1404.
20. Dodds RA, Catterall A, Bitensky L, Chayen J. Effects on fracture healing of an antagonist of the vitamin K cycle. *Calcif Tissue Int.* 1984;36:233-238.
21. Duvall CL, Taylor WR, Weiss D, Wojtowicz AM, Guldberg RE. Impaired angiogenesis, early callus formation, and late stage remodeling in fracture healing of osteopontin-deficient mice. *J Bone Miner Res.* 2007;22:286-297.
22. Einhorn TA. The cell and molecular biology of fracture healing. *Clin Orthop Relat Res.* 1998:S7-21.
23. Eriksson BI, Borris LC, Friedman RJ, Haas S, Huisman MV, Kakkar AK, Bandel TJ, Beckmann H, Muehlhofer E, Misselwitz F, Geerts W. Rivaroxaban versus enoxaparin for thromboprophylaxis after hip arthroplasty. *N Engl J Med.* 2008;358:2765-2775.
24. Eriksson BI, Kakkar AK, Turpie AG, Gent M, Bandel TJ, Homering M, Misselwitz F, Lassen MR. Oral rivaroxaban for the prevention of symptomatic venous thromboembolism after elective hip and knee replacement. *J Bone Joint Surg Br.* 2009;91:636-644.
25. Francis CW, Pellegrini VD, Jr., Totterman S, Boyd AD, Jr., Marder VJ, Liebert KM, Stulberg BN, Ayers DC, Rosenberg A, Kessler C, Johanson NA. Prevention of deep-vein thrombosis after total hip arthroplasty. Comparison of warfarin and dalteparin. *J Bone Joint Surg Am.* 1997;79:1365-1372.
26. Friedlaender GE, Tross RB, Doganis AC, Kirkwood JM, Baron R. Effects of chemotherapeutic agents on bone. I. Short-term methotrexate and doxorubicin (adriamycin) treatment in a rat model. *J Bone Joint Surg Am.* 1984;66:602-607.
27. Gabet Y, Muller R, Regev E, Sela J, Shteyer A, Salisbury K, Chorev M, Bab I. Osteogenic growth peptide modulates fracture callus structural and mechanical properties. *Bone.* 2004;35:65-73.

28. Gajraj NM. The effect of cyclooxygenase-2 inhibitors on bone healing. *Reg Anesth Pain Med.* 2003;28:456-465.

29. Gardner MJ, van der Meulen MC, Demetrakopoulos D, Wright TM, Myers ER, Bostrom MP. In vivo cyclic axial compression affects bone healing in the mouse tibia. *J Orthop Res.* 2006;24:1679-1686.

30. Geiger F, Bertram H, Berger I, Lorenz H, Wall O, Eckhardt C, Simank HG, Richter W. Vascular endothelial growth factor gene-activated matrix (VEGF165-GAM) enhances osteogenesis and angiogenesis in large segmental bone defects. *J Bone Miner Res.* 2005;20:2028-2035.

31. Gigi R, Salai M, Dolkart O, Chechik O, Katzburg S, Stern N, Somjen D. The Effects of Direct Factor Xa Inhibitor (Rivaroxaban) on the Human Osteoblastic Cell Line SaOS2. *Connect Tissue Res.* 2012.

32. Glassman SD, Rose SM, Dimar JR, Puno RM, Campbell MJ, Johnson JR. The effect of postoperative nonsteroidal anti-inflammatory drug administration on spinal fusion. *Spine (Phila Pa 1976).* 1998;23:834-838.

33. Gomez-Outes A, Terleira-Fernandez AI, Suarez-Gea ML, Vargas-Castrillon E. Dabigatran, rivaroxaban, or apixaban versus enoxaparin for thromboprophylaxis after total hip or knee replacement: systematic review, meta-analysis, and indirect treatment comparisons. *BMJ.* 2012;344:e3675.

34. Grundnes O, Reikeras O. The importance of the hematoma for fracture healing in rats. *Acta Orthop Scand.* 1993;64:340-342.

35. Hak DJ, Stewart RL, Hazelwood SJ. Effect of low molecular weight heparin on fracture healing in a stabilized rat femur fracture model. *J Orthop Res.* 2006;24:645-652.

36. Handschin AE, Trentz OA, Hoerstrup SP, Kock HJ, Wanner GA, Trentz O. Effect of low molecular weight heparin (dalteparin) and fondaparinux (Arixtra) on human osteoblasts in vitro. *Br J Surg.* 2005;92:177-183.

37. Hao YJ, Zhang G, Wang YS, Qin L, Hung WY, Leung K, Pei FX. Changes of microstructure and mineralized tissue in the middle and late phase of osteoporotic fracture healing in rats. *Bone.* 2007;41:631-638.

38. Hausman MR, Schaffler MB, Majeska RJ. Prevention of fracture healing in rats by an inhibitor of angiogenesis. *Bone.* 2001;29:560-564.

39. Hazan EJ, Hornicek FJ, Tomford W, Gebhardt MC, Mankin HJ. The effect of adjuvant chemotherapy on osteoarticular allografts. *Clin Orthop Relat Res.* 2001:176-181.

40. Hildebrand T, Ruegsegger P. Quantification of Bone Microarchitecture with the Structure Model Index. *Comput Methods Biomech Biomed Engin.* 1997;1:15-23.

41. Irie A, Takami M, Kubo H, Sekino-Suzuki N, Kasahara K, Sanai Y. Heparin enhances osteoclastic bone resorption by inhibiting osteoprotegerin activity. *Bone.* 2007;41:165-174.

42. Jackson RW, Reed CA, Israel JA, Abou-Keer FK, Garside H. Production of a standard experimental fracture. *Can J Surg.* 1970;13:415-420.

43. Jarvinen TL, Sievanen H, Jokihaara J, Einhorn TA. Revival of bone strength: the bottom line. *J Bone Miner Res.* 2005;20:717-720.

44. Jarvinen TL, Sievanen H, Kannus P, Jarvinen M. Dual-energy X-ray absorptiometry in predicting mechanical characteristics of rat femur. *Bone.* 1998;22:551-558.

45. Jee WS, Park HZ, Roberts WE, Kenner GH. Corticosteroid and bone. *Am J Anat.* 1970;129:477-479.

46. Kanzaki S, Takahashi T, Kanno T, Ariyoshi W, Shinmyouzu K, Tujisawa T, Nishihara T. Heparin inhibits BMP-2 osteogenic bioactivity by binding to both BMP-2 and BMP receptor. *J Cell Physiol.* 2008;216:844-850.

47. Kaspar K, Schell H, Toben D, Matziolis G, Bail HJ. An easily reproducible and biomechanically standardized model to investigate bone healing in rats, using external fixation. *Biomed Tech (Berl).* 2007;52:383-390.

48. Kazakia GJ, Burghardt AJ, Cheung S, Majumdar S. Assessment of bone tissue mineralization by conventional x-ray microcomputed tomography: comparison with synchrotron radiation microcomputed tomography and ash measurements. *Med Phys.* 2008;35:3170-3179.

49. Keller J, Klamer A, Bak B, Suder P. Effect of local prostaglandin E2 on fracture callus in rabbits. *Acta Orthop Scand.* 1993;64:59-63.

50. Khoo DB. The effect of chemotherapy on soft tissue and bone healing in the rabbit model. *Ann Acad Med Singapore.* 1992;21:217-221.

51. Kim SG, Chung TY, Kim MS, Lim SC. The effect of high local concentrations of antibiotics on demineralized bone induction in rats. *J Oral Maxillofac Surg.* 2004;62:708-713.

52. Kock HJ, Werther S, Uhlenkott H, Taeger G. [Influence of unfractionated and low-molecular-weight heparin on bone healing: an animal model]. *Unfallchirurg.* 2002;105:791-796.

53. Krischak GD, Augat P, Sorg T, Blakytny R, Kinzl L, Claes L, Beck A. Effects of diclofenac on periosteal callus maturation in osteotomy healing in an animal model. *Arch Orthop Trauma Surg.* 2007;127:3-9.

54. Lassen MR, Ageno W, Borris LC, Lieberman JR, Rosencher N, Bandel TJ, Misselwitz F, Turpie AG. Rivaroxaban versus enoxaparin for thromboprophylaxis after total knee arthroplasty. *N Engl J Med.* 2008;358:2776-2786.

55. Lassen MR, Gent M, Kakkar AK, Eriksson BI, Homering M, Berkowitz SD, Turpie AG. The effects of rivaroxaban on the complications of surgery after total hip or knee replacement: Results from the RECORD programme. *J Bone Joint Surg Br.* 2012;94:1573-1578.

56. Laux V, Perzborn E, Kubitza D, Misselwitz F. Preclinical and clinical characteristics of rivaroxaban: a novel, oral, direct factor Xa inhibitor. *Semin Thromb Hemost.* 2007;33:515-523.

57. Leonelli SM, Goldberg BA, Safanda J, Bagwe MR, Sethuratnam S, King SJ. Effects of a cyclooxygenase-2 inhibitor (rofecoxib) on bone healing. *Am J Orthop (Belle Mead NJ).* 2006;35:79-84.

58. Leppanen OV, Sievanen H, Jarvinen TL. Biomechanical testing in experimental bone interventions--May the power be with you. *J Biomech.* 2008;41:1623-1631.

59. Luppen CA, Blake CA, Ammirati KM, Stevens ML, Seeherman HJ, Wozney JM, Bouxsein ML. Recombinant human bone morphogenetic protein-2 enhances osteotomy healing in glucocorticoid-treated rabbits. *J Bone Miner Res.* 2002;17:301-310.

60. Ma YF, Li XJ, Jee WS, McOsker J, Liang XG, Setterberg R, Chow SY. Effects of prostaglandin E2 and F2 alpha on the skeleton of osteopenic ovariectomized rats. *Bone.* 1995;17:549-554.

61. Matziolis G, Perka C, Disch A, Zippel H. Effects of fondaparinux compared with dalteparin, enoxaparin and unfractionated heparin on human osteoblasts. *Calcif Tissue Int.* 2003;73:370-379.

62. Mizuno K, Mineo K, Tachibana T, Sumi M, Matsubara T, Hirohata K. The osteogenetic potential of fracture haematoma. Subperiosteal and intramuscular transplantation of the haematoma. *J Bone Joint Surg Br.* 1990;72:822-829.

63. Morgan EF, Mason ZD, Chien KB, Pfeiffer AJ, Barnes GL, Einhorn TA, Gerstenfeld LC. Micro-computed tomography assessment of fracture healing: relationships among callus structure, composition, and mechanical function. *Bone.* 2009;44:335-344.

64. Muir JM, Andrew M, Hirsh J, Weitz JI, Young E, Deschamps P, Shaughnessy SG. Histomorphometric analysis of the effects of standard heparin on trabecular bone in vivo. *Blood.* 1996;88:1314-1320.

65. Muir JM, Hirsh J, Weitz JI, Andrew M, Young E, Shaughnessy SG. A histomorphometric comparison of the effects of heparin and low-molecular-weight heparin on cancellous bone in rats. *Blood.* 1997;89:3236-3242.

66. Muller R, Hildebrand T, Hauselmann HJ, Ruegsegger P. In vivo reproducibility of three-dimensional structural properties of noninvasive bone biopsies using 3D-pQCT. *J Bone Miner Res.* 1996;11:1745-1750.

67. Muller R, Van Campenhout H, Van Damme B, Van Der Perre G, Dequeker J, Hildebrand T, Ruegsegger P. Morphometric analysis of human bone biopsies: a quantitative structural comparison of histological sections and micro-computed tomography. *Bone.* 1998;23:59-66.

68. Nazarian A, Snyder BD, Zurakowski D, Muller R. Quantitative micro-computed tomography: a non-invasive method to assess equivalent bone mineral density. *Bone.* 2008;43:302-311.

69. Nelson-Piercy C, Letsky EA, de Swiet M. Low-molecular-weight heparin for obstetric thromboprophylaxis: experience of sixty-nine pregnancies in sixty-one women at high risk. *Am J Obstet Gynecol.* 1997;176:1062-1068.

70. Nyman JS, Munoz S, Jadhav S, Mansour A, Yoshii T, Mundy GR, Gutierrez GE. Quantitative measures of femoral fracture repair in rats derived by micro-computed tomography. *J Biomech.* 2009;42:891-897.

71. Osip SL, Butcher M, Young E, Yang L, Shaughnessy SG. Differential effects of heparin and low molecular weight heparin on osteoblastogenesis and adipogenesis in vitro. *Thromb Haemost.* 2004;92:803-810.

72. Park SH, Silva M, Bahk WJ, McKellop H, Lieberman JR. Effect of repeated irrigation and debridement on fracture healing in an animal model. *J Orthop Res.* 2002;20:1197-1204.

73. Parker MJ, Raghavan R, Gurusamy K. Incidence of fracture-healing complications after femoral neck fractures. *Clin Orthop Relat Res.* 2007;458:175-179.

74. Perry AC, Prpa B, Rouse MS, Piper KE, Hanssen AD, Steckelberg JM, Patel R. Levofloxacin and trovafloxacin inhibition of experimental fracture-healing. *Clin Orthop Relat Res.* 2003:95-100.

75. Perzborn E, Kubitza D, Misselwitz F. Rivaroxaban. A novel, oral, direct factor Xa inhibitor in clinical development for the prevention and treatment of thromboembolic disorders. *Hamostaseologie.* 2007;27:282-289.

76. Perzborn E, Roehrig S, Straub A, Kubitza D, Mueck W, Laux V. Rivaroxaban: a new oral factor Xa inhibitor. *Arterioscler Thromb Vasc Biol.* 2010;30:376-381.

77. Pountos I, Corscadden D, Emery P, Giannoudis PV. Mesenchymal stem cell tissue engineering: techniques for isolation, expansion and application. *Injury.* 2007;38 Suppl 4:S23-33.

78. Pountos I, Georgouli T, Blokhuis TJ, Pape HC, Giannoudis PV. Pharmacological agents and impairment of fracture healing: what is the evidence? *Injury.* 2008;39:384-394.

79. Puzas JE, O'Keefe RJ, Schwarz EM, Zhang X. Pharmacologic modulators of fracture healing: the role of cyclooxygenase inhibition. *J Musculoskelet Neuronal Interact.* 2003;3:308-312; discussion 320-301.

80. Radi ZA, Khan NK. Effects of cyclooxygenase inhibition on bone, tendon, and ligament healing. *Inflamm Res.* 2005;54:358-366.

81. Rajgopal R, Bear M, Butcher MK, Shaughnessy SG. The effects of heparin and low molecular weight heparins on bone. *Thromb Res.* 2008;122:293-298.

82. Reuben SS, Ablett D, Kaye R. High dose nonsteroidal anti-inflammatory drugs compromise spinal fusion. *Can J Anaesth.* 2005;52:506-512.

83. Roehrig S, Straub A, Pohlmann J, Lampe T, Pernerstorfer J, Schlemmer KH, Reinemer P, Perzborn E. Discovery of the novel antithrombotic agent 5-chloro-N-({(5S)-2-oxo-3- [4-(3-oxomorpholin-4-yl)phenyl]-1,3-oxazolidin-5-yl}methyl)thiophene- 2-carboxamide (BAY 59-7939): an oral, direct factor Xa inhibitor. *J Med Chem.* 2005;48:5900-5908.

84. Schmidhammer R, Zandieh S, Mittermayr R, Pelinka LE, Leixnering M, Hopf R, Kroepfl A, Redl H. Assessment of bone union/nonunion in an experimental model using microcomputed technology. *J Trauma.* 2006;61:199-205.

85. Shaughnessy SG, Hirsh J, Bhandari M, Muir JM, Young E, Weitz JI. A histomorphometric evaluation of heparin-induced bone loss after discontinuation of heparin treatment in rats. *Blood.* 1999;93:1231-1236.

86. Shaughnessy SG, Young E, Deschamps P, Hirsh J. The effects of low molecular weight and standard heparin on calcium loss from fetal rat calvaria. *Blood.* 1995;86:1368-1373.

87. Shefelbine SJ, Simon U, Claes L, Gold A, Gabet Y, Bab I, Muller R, Augat P. Prediction of fracture callus mechanical properties using micro-CT images and voxel-based finite element analysis. *Bone.* 2005;36:480-488.

88. Shuid AN, Mohamad S, Mohamed N, Fadzilah FM, Mokhtar SA, Abdullah S, Othman F, Suhaimi F, Muhammad N, Soelaiman IN. Effects of calcium supplements on fracture healing in a rat osteoporotic model. *J Orthop Res.* 2010;28:1651-1656.

89. Solayar GN, Walsh PM, Mulhall KJ. The effect of a new direct Factor Xa inhibitor on human osteoblasts: an in-vitro study comparing the effect of rivaroxaban with enoxaparin. *BMC Musculoskelet Disord.* 2011;12:247.

90. Sommer-Tsilenis E, Sauer HD, Kruse HP. Delaying effect of cyclophosphamide on bone fracture healing chemical analyses of rat femora. *Arch Orthop Trauma Surg.* 1983;101:89-93.

91. Squires JW, Pinch LW. Heparin-induced spinal fractures. *JAMA.* 1979;241:2417-2418.

92. Stinchfield FE, Sankaran B, Samilson R. The effect of anticoagulant therapy on bone repair. *J Bone Joint Surg Am.* 1956;38-A:270-282.

93. Street J, Winter D, Wang JH, Wakai A, McGuinness A, Redmond HP. Is human fracture hematoma inherently angiogenic? *Clin Orthop Relat Res.* 2000:224-237.

94. Street JT, McGrath M, O'Regan K, Wakai A, McGuinness A, Redmond HP. Thromboprophylaxis using a low molecular weight heparin delays fracture repair. *Clin Orthop Relat Res.* 2000:278-289.

95. Tuncay I, Ozbek H, Kosem M, Unal O. A comparison of effects of fluoroquinolones on fracture healing (an experimental study in rats). *Ulus Travma Acil Cerrahi Derg.* 2005;11:17-22.

96. Turner CH, Burr DB. Basic biomechanical measurements of bone: a tutorial. *Bone.* 1993;14:595-608.

97. Turpie AG. Efficacy of a postoperative regimen of enoxaparin in deep vein thrombosis prophylaxis. *Am J Surg.* 1991;161:532-536.

98. Walenga JM, Bick RL. Heparin-induced thrombocytopenia, paradoxical thromboembolism, and other side effects of heparin therapy. *Med Clin North Am.* 1998;82:635-658.

99. Wawrzynska L, Tomkowski WZ, Przedlacki J, Hajduk B, Torbicki A. Changes in bone density during long-term administration of low-molecular-weight heparins or acenocoumarol for secondary prophylaxis of venous thromboembolism. *Pathophysiol Haemost Thromb.* 2003;33:64-67.

100. Yamaji T, Ando K, Wolf S, Augat P, Claes L. The effect of micromovement on callus formation. *J Orthop Sci.* 2001;6:571-575.

101. Zhang J, Weir V, Fajardo L, Lin J, Hsiung H, Ritenour ER. Dosimetric characterization of a cone-beam O-arm imaging system. *J Xray Sci Technol.* 2009;17:305-317.